Power Optimization of Cell-Free Massive MIMO With Full-Duplex and Low-Resolution ADCs

Prince Anokye, Derek Kwaku Pobi Asiedu, Kyoung-Jae Lee

Power Optimization of Cell-Free Massive MIMO With Full-Duplex and Low-Resolution ADCs

Prince Anokye, *Member, IEEE*, Derek K. P. Asiedu, *Member, IEEE*, and Kyoung-Jae Lee, *Senior Member, IEEE*

***Abstract*—This paper analyzes the spectral/energy efficiency (SE/EE) of a full-duplex (FD) cell-free (CF) massive multiple-input multiple-output (mMIMO) over Rician fading channels. Due to the FD radios, the access points (APs) suffer from self-interference (SI) and inter-AP interference (IAI) while the downlink (DL) users' signals are corrupted by the uplink (UL) users' transmissions. We consider the case, where low-resolution analog-to-digital converters (ADCs) are utilized at the APs and DL users, which introduces the quantization noise (QN). The combined effects of Rician κ-factor, residual SI/IAI, UL-to-DL interference, multi-user interference, and QN on the UL/DL SEs are characterized. The UL SE is degraded by the increase in DL power, whereas the growth in UL power deteriorates the DL SE. The effects of the residual SI/IAI and UL-to-DL interference are worsened by the low-resolution ADCs. We optimize the UL/DL transmit powers to maximize the overall sum SE of the network. It is observed that the proposed power allocation algorithm brings substantial sum SE gain. A trade-off analysis between the EE and SE, as a function of the ADCs' resolution, shows that the entire envelope of the operating region of FD CF mMIMO is enhanced in Rician channels.**

***Index Terms*—Full-duplex, cell-free massive multiple-input multiple-output, low-resolution analog-to-digital converters, sum spectral efficiency maximization.**

I. Introduction

THE cell-free (CF) massive multiple-input multiple-output (mMIMO), which is a scalable implementation of the distributed antenna system (DAS), has received significant attention in the literature as enabling technology for beyond fifth-generation (5G) and 6G communication systems. In CF mMIMO, a large number of access points (APs) are distributed over a wide geographical area and connected to central processing units (CPUs) via backhaul links to serve fewer users jointly. The CF mMIMO inherits the benefits of both DASs (i.e., to provide macro-diversity against shadow fading [1]) and cellular mMIMO (i.e., to exploit favorable propagation and channel hardening [2]). Since the APs are closer to the users, the CF mMIMO promises a higher coverage probability compared to the cellular mMIMO. Furthermore, there are no cell boundaries, hence, handovers are avoided and users achieve uniformly good quality-of-service (QoS). The authors of [3] study the CF mMIMO, where it is shown that the CF mMIMO offers a five-fold improvement in the 95%-likely per-user throughput than the small-cell system. The energy efficiency (EE) maximization problem is investigated by assuming the maximum ratio transmission (MRT) in [4] and zero-forcing (ZF) precoding in [5]. Considering phase-shifts in Rician channels, [6] derives uplink/downlink (UL/DL) SE expressions for phase-aware minimum mean square error (MMSE), linear MMSE, and least square estimators. The work [7] extends [6] by considering the element-wise MMSE channel estimator. The deduction made from [3]–[7] is that CF mMIMO provides SE/EE improvement over conventional cellular systems.

Another major technology earmarked for next-generation systems is the in-band full-duplex (FD). By allowing the UL and DL transmissions to occur simultaneously on the same time-frequency resources, FD has the capability to recover the bandwidth loss inherent in traditional half-duplex (HD) systems. The major problem inhibiting the implementation of FD is the self-interference (SI) which occurs due to the signal leakage from the transmit to the receive radio frequency (RF) chains of the same terminal [8]. Considering recent advances in SI cancellation methods [9], i.e., bringing the SI power to the background noise level, incorporating FD in the modern wireless infrastructure is a practical solution to enhance the SE. Thus, combining the FD and CF mMIMO with the aim of exploiting the full benefits of the two technologies is only a natural consequence. Nonetheless, only a few papers have investigated the FD and CF mMIMO [10]–[12]. The work [10] derives the closed-form solutions for the UL/DL SE by assuming imperfect channel state information (CSI) and maximum ratio combining (MRC)/MRT. Here, it is shown that residual SI and inter-AP interference (IAI) remain key constraints. In [11], the network-assisted FD CF mMIMO is considered such that an AP performs either transmission, reception or simultaneous transmission and reception based on the network load. To suppress the SI/IAI and UL-to-DL interference, the MMSE and regularized ZF are used. The SE/EE maximization problem of the FD CF mMIMO is considered in [12], where the power control, AP-user association, and AP selection are jointly optimized. The optimization problem is solved based on the instantaneous CSI. Therefore, the optimal solutions have to be re-calculated during every coherence interval which is computationally intensive and increases the backhaul traffic. The works [10]–[12] confirm that the FD CF mMIMO offers substantial gains in terms of SE/EE relative to the HD mode. The common assumption in [10]–[12] is that the FD CF mMIMO operates over Rayleigh distributed channels and perfect hardware is used at the APs and users.

P. Anokye and K. -J. Lee are with the Department of Electronics Engineering, Hanbat National University, Daejeon 34158, South Korea. (Email: princemcanokye@yahoo.com, kyoungjae@hanbat.ac.kr).

D. K. P. Asiedu is with the Department of Mathematics and Electrical Engineering, Institut Mines-Telecom (IMT) Atlantique, Brest 29238, France. (Email:kwakupobi@gmail.com).

Corresponding Author: Kyoung-Jae Lee

The FD CF mMIMO increases the power consumed in the network since additional APs and by extension more RF chains are deployed. This poses major challenges to the global climate and electricity cost for network operators. For MIMO systems, the analog-to-digital converters (ADCs) remain key power consumption impediment [13]. A typical receive antenna has a pair of ADCs to quantize the real and quadrature components of a signal. To elaborate, an ADC with resolution b and sampling frequency f_s performs $2^b f_s$ computations per second, i.e., the power dissipation increases linearly with f_s and exponentially with b [14].[1] Furthermore, the financial cost of the ADC fabrication grows with the resolution. Thus, for practical implementation of FD CF mMIMO, the ADCs power consumption must be scaled down. A promising solution is to use low-resolution ADCs. For example, in a network, power-constrained mobile users could consider combining with low-resolution ADCs in the DL, to reduce power. However, coarse quantization with low-resolution ADCs leads to the quantization noise (QN) whose strength grows proportionally with the received signal power. Therefore, to use low-resolution ADCs in FD CF mMIMO, proper investigation to ascertain its feasibility must be conducted.

Recently, CF mMIMO with low-resolution ADCs has been studied by [15], [17]–[20]. With low-resolution ADCs at the APs and DL users over Rayleigh channels, [15] derives the closed-form solution for the DL rate and proposes a max-min algorithm to ensure uniformly good QoS. Zhang et al. [19] assume Rician channels and derive approximate rate expressions for the CF mMIMO with low-resolution ADCs at the APs only. An UL SE expression for the CF mMIMO with mixed-ADCs is derived in [20]. The works [15], [19], [20] model the low-resolution ADC receiver via the additive quantization noise model (AQNM). Using the Bussgang Theorem, [17] jointly optimizes the pilot sequence and analog filters with one-bit ADCs at the APs while [18] analyzes the one-bit ADCs impact on the CSI quality. The aforementioned works are based on the HD setting and are not directly applicable to the FD mode since the FD CF mMIMO is more complicated due to the residual SI/IAI and UL-to-DL interference. Moreover, as observed in the co-located FD mMIMO [21], [22], the SI effect is worsened by the use of low-resolution ADCs. The article [16] investigates the SE/EE of an FD CF mMIMO with low-resolution ADCs but [16] is limited to Rayleigh channels and the power allocation problem is not considered.

Motivated by the above, this article studies the performance of the FD CF mMIMO over Rician fading channels. Each AP possesses FD radios, where transmission and reception occurs simultaneously on the same time-frequency resources. This results in the SI and IAI phenomenon at the APs and the UL-to-DL interference at the DL users. To reduce the power consumption of the network, low-resolution ADCs are utilized not only at the APs but also at the DL users. This leads to the QN at both the APs and DL users. To alleviate the SE degradation due to residual SI/IAI, UL-to-DL interference, and QN, we propose an efficient power allocation algorithm to improve the total sum SE. The main contributions of this paper are summarized as follows:

- Considering FD APs and HD users, we characterize the joint impact of QN, residual SI/IAI, and UL-to-DL interference by deriving closed-form expressions for the achievable UL/DL SEs. The closed-form solutions enable us to study the influence of the APs, Rician κ-factor, ADCs resolution, residual SI/IAI, and UL-to-DL interference. It is shown that the UL SE loss as a result of the QN can be compensated by increasing APs. However, in the DL, the desired signal and QN have equal order in the number of APs. Thus, the DL SE saturates rapidly as the APs increase. We show that in pure line-of-sight (LoS) environments, the UL and DL SEs converge to fixed values, irrespective of the channel estimation quality.
- We consider the sum SE maximization subject to the per AP and UL user power constraints. Due to the non-convexity of the problem, the equivalent relationship between the sum SE maximization and the weighted MMSE (WMMSE) minimization problems is exploited to develop iterative algorithm based on the alternating optimization framework. From the results, the proposed power allocation algorithm provides significant gains in the sum SE (of the FD CF mMIMO with low-resolution ADCs) relative to the setup with uniform power.
- A trade-off analysis between the EE and SE as a function of the ADCs' resolution, is performed. The EE grows initially as the quantization bits increase but EE declines beyond a certain threshold. The optimal resolution that maximizes the EE can be numerically obtained.

The rest of the paper is organized as follows: Section II discusses the system model. In Section III, we present SE expressions and derive closed-form solutions for the UL/DL SEs. Section IV studies the UL/DL power allocation problem. EE and numerical results are discussed in Section V. Section VI concludes the paper.

Notations: Bold face lower case and upper case letters represent vectors and matrices, respectively. $\mathbb{E}\{\cdot\}$, $\text{Var}(\cdot)$, and $(\cdot)^H$ denote the expectation, variance and Hermitian operators, respectively. $\mathbf{a} \sim \mathbb{CN}(\mathbf{0}, \mathbf{A})$ indicates a circularly symmetric complex Gaussian random variable with mean $\mathbf{0}$ and covariance $\mathbf{A}$. $\text{diag}(\mathbf{A})$ returns the diagonal entries of $\mathbf{A}$. $[\mathbf{A}]_{mn}$ denotes an element on the m-th row and n-th column of $\mathbf{A}$.

II. System Model

Consider an FD CF mMIMO system in Fig. 1, where M multi-antenna APs serve single antenna L_u UL users and L_d DL users. The APs are connected together to a CPU via error-free and limitless-capacity backhaul links. Each FD AP has N_{rx} receive and N_{tx} transmit antennas. The users operate in HD mode. Since the APs transmit and receive on the

[1]For FD systems with separate antenna configuration, ADCs are required at both the receive and transmit antenna chains for quantizing the received UL pilots during the channel estimation phase. It is noted in [14] that digital-to-analog converters (DACs) consume less power. Hence, this article only focuses on the receiver structures with ADCs as it is done in [15], [16].

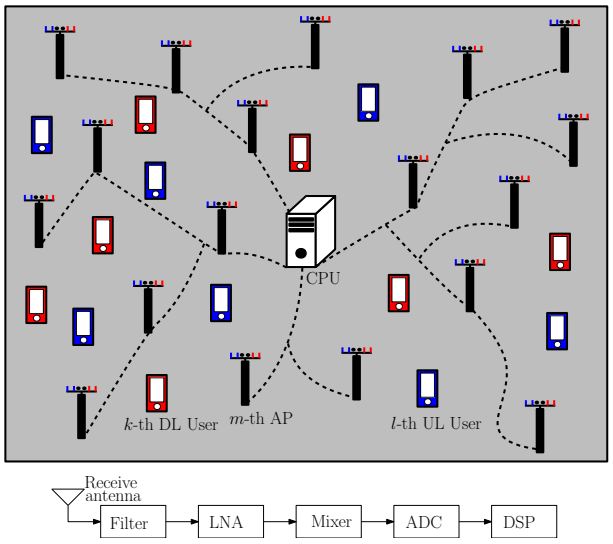

Fig. 1: FD CF mMIMO network, where there are M APs, L_u UL users and L_d DL users.

same frequency, the APs suffer from the SI and IAI. Because the DL users receive on the same frequency on which the UL users transmit, the signals received at the DL users are corrupted by UL transmissions which results in the UL-to-DL interference. Also, the receive antennas at each AP and DL user are equipped with low-resolution ADCs to reduce power consumption. Because of the low-resolution ADCs, QN is introduced into the received signals. We assume the standard block fading, where the channel response is flat for a given coherence interval τ_c. For each τ_c, τ_p time slot are reserved for UL piloting while the remaining slot, i.e., $\tau_s = \tau_c - \tau_p$, are for useful data. Assuming the time division duplex protocol, the CSI acquired via UL pilot signaling are used to precode the DL signal, i.e., we assume perfect hardware calibration such that reciprocity holds [23]. Further, we follow the general assumption that the input signals are Gaussian distributed.

A. Channel Model

Let the channels from the l-th UL and k-th DL users to the m-th AP as $\mathbf{h}_{ml} \in \mathbb{C}^{N_{rx}\times 1}$ and $\mathbf{g}_{mk} \in \mathbb{C}^{N_{tx}\times 1}$, respectively. We assume uncorrelated Rician fading channels since it covers more scenarios than the Rayleigh such as conditions where line-of-sight (LoS) exists between the APs and users. A typical example is millimeter wave applications. Future work will consider the impact of channel correlation. Thus, the channels are modeled as [24],

$$\mathbf{g}_{mk} = \mathbf{g}_{L,mk}\kappa_{mk}^{1/2}\bar{\kappa}_{mk}^{-1/2} + \mathbf{g}_{w,mk}\bar{\kappa}_{mk}^{-1/2},$$
$$\mathbf{h}_{ml} = \mathbf{h}_{L,ml}\kappa_{ml}^{1/2}\bar{\kappa}_{ml}^{-1/2} + \mathbf{h}_{w,ml}\bar{\kappa}_{ml}^{-1/2},$$

where $\mathbf{g}_{L,mk} = \beta_{mk}^{1/2}\bar{\mathbf{g}}_{L,mk}$ and $\mathbf{g}_{w,mk} = \beta_{mk}^{1/2}\bar{\mathbf{g}}_{w,mk}$ denote the deterministic LoS and random Rayleigh components of $\mathbf{g}_{mk}$, respectively; β_{mk} indicates the large-scale fading coefficient between the m-th AP and k-th DL user which comprises the pathloss and shadow fading effects. The large-scale fading coefficients remain unchanged over several coherence intervals. $\bar{\mathbf{g}}_{w,mk}$ describes the small-scale fading whose elements are modeled as $\mathbb{CN}(0,1)$. κ_{mk} indicate Rician κ-factor and $\bar{\kappa}_{mk} \triangleq \kappa_{mk} + 1$.[2] Also, $[\bar{\mathbf{g}}_{L,mk}]_n = e^{-j(n-1)(2\pi d/\lambda)\sin(\psi_{mk}^d)}$, where d, λ, and ψ_{mk}^d denote the antenna spacing, wavelength, and angle of arrival (AoA) from the k-th DL user to the m-th AP, respectively. Similarly, for the UL channel, $\mathbf{h}_{L,ml} = \zeta_{ml}^{1/2}\bar{\mathbf{h}}_{L,ml}$ and $\mathbf{h}_{w,ml} = \zeta_{ml}^{1/2}\bar{\mathbf{h}}_{w,ml}$ represent the deterministic LoS and random Rayleigh components, respectively. ζ_{ml} indicates the large-scale fading coefficient from the m-th AP to the l-th UL user and $\bar{\mathbf{h}}_{w,ml}$ denotes the small-scale fading vector whose elements are distributed as $\mathbb{CN}(0,1)$. κ_{ml} is the Rician κ-factor and $\bar{\kappa}_{ml} = \kappa_{ml} + 1$. We have $[\bar{\mathbf{h}}_{L,ml}]_n = e^{-j(n-1)(2\pi d/\lambda)\sin(\psi_{ml}^u)}$, where ψ_{ml}^u is the AoA from the l-th UL user to m-th AP. Without loss of generality, let $d = \lambda/2$.

B. Channel Estimation

To precode the DL signal and decode the UL data, the APs need to acquire local CSI. In this paper, we assume that only imperfect CSI is available. The estimates of $\mathbf{g}_{mk}$ and $\mathbf{h}_{ml}$ are obtained at the APs via the linear MMSE (LMMSE) method. For the Rician channel, we consider that the LoS parts are known a priori and we only estimate the Rayleigh component. Since the LoS components change much slowly, classical estimation methods such as MUSIC [25] which uses the signal subspace and ESPRIT [26] which exploits the rotational invariance among signal subspaces can be employed to accurately estimate the LoS parameters. The common assumption in the literature is that the LoS is perfectly known [22], [24], [27]. That notwithstanding, the LoS estimation may be imperfect and a lower bound on the achievable SE of the system can be derived under the assumption that the LoS parts are completely unknown— we do not pursue this analysis herein because of space limitations. Thus, the estimates of the k-th DL and l-th UL users' true channels are given, respectively, as

$$\hat{\mathbf{g}}_{mk} = \mathbf{g}_{L,mk}\kappa_{mk}^{1/2}\bar{\kappa}_{mk}^{-1/2} + \hat{\mathbf{g}}_{w,mk}\bar{\kappa}_{mk}^{-1/2}, \quad (1)$$
$$\hat{\mathbf{h}}_{ml} = \mathbf{h}_{L,ml}\kappa_{ml}^{1/2}\bar{\kappa}_{ml}^{-1/2} + \hat{\mathbf{h}}_{w,ml}\bar{\kappa}_{ml}^{-1/2}, \quad (2)$$

where $\hat{\mathbf{g}}_{w,mk}$ and $\hat{\mathbf{h}}_{w,ml}$ denote the estimated Rayleigh components.

To estimate the random components, the DL users transmit their pilot sequences to the APs while the UL users remain silent. After that, the UL users send their pilots to the APs while the DL users keep silent. We assume that mutually orthogonal pilot sequences are employed to avoid pilot contamination[3] and low-resolution ADCs are used at the APs for channel estimation. Without loss of generality, we assume that the same resolution ADCs are used at the m-th AP's receive and transmit arrays for quantizing the received pilot signals. The estimates $\hat{\mathbf{g}}_{w,mk}$ and $\hat{\mathbf{h}}_{w,ml}$ are obtained by following [16]. Defining $\tilde{\mathbf{g}}_{mk}$ and $\tilde{\mathbf{h}}_{ml}$ as the estimation errors, the true channels can be decomposed as $\mathbf{g}_{mk} = \hat{\mathbf{g}}_{mk} + \tilde{\mathbf{g}}_{mk}$ and

[2]The Rician κ-factor measures the ratio of the power of the deterministic LoS component to the scattered components [24].

[3]To achieve mutual orthogonality, the DL pilot length $\tau_d \geq L_d$ and for the UL pilot length $\tau_u \geq L_u$. Therefore, $\tau_p = \tau_d + \tau_u$.

$\mathbf{h}_{ml} = \hat{\mathbf{h}}_{ml} + \tilde{\mathbf{h}}_{ml}$. From the properties of LMMSE estimation, $\hat{\mathbf{g}}_{mk} \sim \mathbb{CN}(\mathbb{E}\{\hat{\mathbf{g}}_{mk}\}, \hat{\beta}_{mk}\mathbf{I}_{N_{tx}})$ and $\tilde{\mathbf{g}}_{mk} \sim \mathbb{CN}(0, \tilde{\beta}_{mk}\mathbf{I}_{N_{tx}})$ are mutually independent [27], where $\hat{\beta}_{mk} = \beta_{mk}\nu_{mk}\bar{\kappa}_{mk}^{-1}$ and $\nu_{mk} = p_\tau\tau_d\alpha_m\beta_{mk}/(1 + p_\tau\tau_d\beta_{mk})$ with $\tilde{\beta}_{mk} = \beta_{mk}\bar{\kappa}_{mk}^{-1} - \hat{\beta}_{mk}$. Similarly, $\hat{\mathbf{h}}_{ml} \sim \mathbb{CN}(\mathbb{E}\{\hat{\mathbf{h}}_{ml}\}, \hat{\zeta}_{ml}\mathbf{I}_{N_{rx}})$ and $\tilde{\mathbf{h}}_{ml} \sim \mathbb{CN}(0, \tilde{\zeta}_{mk}\mathbf{I}_{N_{rx}})$, where $\hat{\zeta}_{ml} = \zeta_{ml}\mu_{ml}\bar{\kappa}_{ml}^{-1}$, $\mu_{ml} = p_\tau\tau_u\alpha_m\zeta_{ml}/(1 + p_\tau\tau_u\zeta_{ml})$, and $\tilde{\zeta}_{ml} = \zeta_{ml}\bar{\kappa}_{ml}^{-1} - \hat{\zeta}_{ml}$. p_τ denotes the pilot power and α_m describes the ADCs resolution at the APs' transmit/receive antennas.

C. Uplink Data Transmission

The L_u UL users send data to the APs. Simultaneously, each AP sends data to the DL users. This leads to the SI and IAI at the m-th AP. The signal received at the m-th AP is given by

$$\mathbf{y}_m^u = \sum_{l=1}^{L_u} \mathbf{h}_{ml}\sqrt{p_{u,l}}s_l^u + \sum_{n=1}^{M} \mathbf{Q}_{mn}\mathbf{x}_n^d + \mathbf{z}_m,$$

where $p_{u,l}$ denotes the l-th UL user power and $0 \leq p_{u,l} \leq P_{u,l}^{MAX}$; $P_{u,l}^{MAX}$ is the maximum power available at the l-th UL user. $s_l^u \sim \mathbb{CN}(0,1)$ represents the l-th UL user data. Also, $\mathbf{z}_m \in \mathbb{C}^{N_{rx}\times 1}$ and $\mathbf{x}_n \in \mathbb{C}^{N_{tx}\times 1}$ denote the noise at the m-th AP and n-th AP transmit signal, respectively. The elements of $\mathbf{z}_m$ are modeled by $\mathbb{CN}(0,1)$. $\mathbf{Q}_{mn} \in \mathbb{C}^{N_{rx}\times N_{tx}}$ represents the residual SI/IAI channel from the n-th AP to the m-th AP whose elements are $\mathbb{CN}(0, \rho_{mn})$, where $\rho_{mn} = \rho_{SI}^2\sigma_{AP,mn}$; $\sigma_{AP,mn}$ denote the large-scale fading from the n-th AP to m-th AP and ρ_{SI}^2 is the residual interference after SI suppression [10]. Considering a CF mMIMO, thanks to the fact that the UL and DL signals are centrally processed, some form of digital interference cancellation can be realized [11]. Moreover, the SI is canceled at the local AP such that any residual interference originating from the imperfect cancellation is regarded as additional noise. Again, by properly separating the transmit and receive antenna arrays, natural isolation occurs such that the surrounding buildings or shielding plates are exploited to suppress the LoS component. The common assumption is to model this as Rayleigh [8], [10], [28].

The m-th AP quantizes the received signal before digital processing. The low-resolution ADC receiver is modeled by considering the non-uniform quantizer, where the quantization error is approximated as a linear gain with the AQNM. We note that the AQNM has been shown in [29], [30] to be accurate enough for MIMO channels, especially at the low and medium signal-to-noise ratio (SNR) regimes, where our system is expected to operate. Further, the AQNM has been extensively employed in the quantized MIMO systems for performance analysis and power optimization [15], [20], [31], [32]. Thus, the quantizer output at the m-th AP is written as

$$\tilde{\mathbf{y}}_m^u = \alpha_m\mathbf{y}_m^u + \tilde{\mathbf{z}}_m,$$

where $\alpha_m = 1 - \xi$ and ξ relates to the ADC resolution b_m^{AP}. Approximate values of ξ for $b_m^{AP} \leq 5$ are shown in [22, Table I]. For $b_m^{AP} > 5$, $\xi = \frac{\pi\sqrt{3}}{2} \cdot 2^{-2b_m^{AP}}$. Also, $\tilde{\mathbf{z}}_m \sim \mathbb{CN}(\mathbf{0}, \mathbf{R}_{\tilde{\mathbf{z}}_m})$ denotes the additive QN whose covariance is defined by $\mathbf{R}_{\tilde{\mathbf{z}}_m} = (\alpha_m - \alpha_m^2)\text{diag}(\mathbb{E}\{\mathbf{y}^u(\mathbf{y}^u)^H\})$. After quantization, the m-th AP applies the receive filter before forwarding the signal to the CPU. We assume the MRC/MRT due to its computational simplicity and can be implemented in a distributed fashion [3].[4] Thus, the l-th UL user's signal "seen" by the CPU is expressed by

$$\tilde{y}_l^u = \sum_{m=1}^{M} \hat{\mathbf{h}}_{ml}^H\tilde{\mathbf{y}}_m^u. \tag{3}$$

D. Downlink Data Transmission

For the DL, the APs precode the signals intended for the L_d DL users.[5] The signal received at the k-th DL user is corrupted by the signals transmitted by the UL users. The m-th AP transmits the signal $\mathbf{x}_m^d = \sum_{k=1}^{L_d}\sqrt{\eta_{mk}}\hat{\mathbf{g}}_{mk}s_k^d$, where $s_k^d \sim \mathbb{CN}(0,1)$ and η_{mk} are the k-th DL data and power allocation coefficient from the m-th AP to the k-th DL user, respectively. For the per AP power constraint to be met, $N_{tx}\sum_{k=1}^{L_d}\eta_{mk}a_{mk}^d \leq P_{d,m}^{MAX}$, where $P_{d,m}^{MAX}$ denotes the available power and $a_{mk}^d \triangleq \beta_{mk}\bar{\kappa}_{mk}^{-1}(\kappa_{mk} + \nu_{mk})$. The received signal at the k-th DL user is written as

$$y_k^d = \sum_{k'=1}^{L_d}\sum_{m=1}^{M}\sqrt{\eta_{mk'}}\mathbf{g}_{mk}^H\hat{\mathbf{g}}_{mk'}s_{k'}^d + \sum_{l=1}^{L_u}\sqrt{p_{u,l}}q_{kl}s_l^u + z_k^d,$$

where $z_k^d \sim \mathbb{CN}(0,1)$ and $q_{kl} \sim \mathbb{CN}(0, \gamma_{kl}^2)$ indicates the noise and UL-to-DL interference channel from the l-th UL user to the k-th DL user, respectively. Similarly, $\gamma_{kl}^2 = \sigma_{UE,kl}\rho_{SI}^2$, where $\sigma_{UE,kl}$ indicates the large-scale fading between the l-th UL user and the k-th DL user. The k-th DL user quantizes the received signal and the quantizer output is expressed as $\tilde{y}_k^d = \varepsilon_k y_k^d + \tilde{z}_k^d$, where $\varepsilon_k = 1 - \xi$ and $\tilde{z}_k^d \sim \mathbb{CN}(0, \tilde{Z}_k^d)$ describe the ADC resolution and additive QN, respectively. Also, $\tilde{Z}_k^d = (\varepsilon_k - \varepsilon_k^2)\mathbb{E}\{|y_k^d|^2\}$. For the ADCs resolution b_k^{UE} at the k-th DL user, ξ is obtained as in Section II-C. The next section analyzes the UL/DL SE of the system.

III. Spectral Efficiency Analysis

To derive the SE, we employ the "use-and-then-forget" (UaTF) method, where the received signal is rewritten as a known mean gain plus an uncorrelated additive noise [3].

[4]ZF and MMSE are other linear processing methods which may improve the system performance by suppressing multi-user interference (MUI) and residual SI/IAI [33]. Recently, the nonlinear method named ZF-group successive interference cancellation (GSIC) has also been proposed in [34] to improve the EE of the HD co-located mMIMO with low-resolution ADCs. Considering the intensive deployment of APs in the FD CF mMIMO, this potential improvement due to fully centralized processing methods such as ZF, MMSE, ZF-GSIC, and MMSE-GSIC may come at the cost of higher computational complexity and backhaul traffic. A future work will analyze the trade-off between the system performance and complexity.

[5]The CPU connecting all the APs controls the information exchange such as data payload and power control coefficients while the APs are responsible for locally acquiring the CSI and precoding.

Specifically, the signal for the l-th UL user, i.e., (3) is rewritten as

$$\tilde{y}_l^u = \sqrt{p_{u,l}}\mathbb{E}\Big\{\sum_{m=1}^{M}\alpha_m\hat{\mathbf{h}}_{ml}^H\mathbf{h}_{ml}\Big\}s_l^u + \sqrt{p_{u,l}}\Big(\sum_{m=1}^{M}\alpha_m\hat{\mathbf{h}}_{ml}^H\mathbf{h}_{ml} - \mathbb{E}\Big\{\sum_{m=1}^{M}\alpha_m\hat{\mathbf{h}}_{ml}^H\mathbf{h}_{ml}\Big\}\Big)s_l^u + \sum_{l'\neq l}^{L_u}\sum_{m=1}^{M}\sqrt{p_{u,l'}}\alpha_m\hat{\mathbf{h}}_{ml}^H\mathbf{h}_{ml'}s_{l'}^u + \sum_{m=1}^{M}\sum_{n=1}^{M}\alpha_m\hat{\mathbf{h}}_{ml}^H\mathbf{Q}_{mn}\mathbf{x}_n + \sum_{m=1}^{M}\alpha_m\hat{\mathbf{h}}_{ml}^H\mathbf{z}_m + \sum_{m=1}^{M}\hat{\mathbf{h}}_{ml}^H\tilde{\mathbf{z}}_m,$$

where the first term denotes the desired signal and the remaining terms represent the effective noise which are uncorrelated. The lower bound on the achievable SE is acquired by adopting the concept that the additive Gaussian noise is the worst-case uncorrelated noise. Thus, the achievable SE for the l-th UL user is given by

$$R_l^u = \frac{\tau_s}{\tau_c}\log_2\left(1 + \frac{p_{u,l}|\mathbb{E}\{\sum_{m=1}^{M}\alpha_m\hat{\mathbf{h}}_{ml}^H\mathbf{h}_{ml}\}|^2}{B_l^u + C_{ll'}^u + D_l^u + E_l^u + F_l^u}\right), \quad (4)$$

where B_l^u, C_l^u, D_l^u, E_l^u, and F_l^u denote the power of beamforming uncertainty gain (BUG), MUI, residual SI/IAI, noise, and QN, respectively. We define

$$B_l^u \triangleq p_{u,l}\text{Var}\Big(\sum_{m=1}^{M}\alpha_m\hat{\mathbf{h}}_{ml}^H\mathbf{h}_{ml}\Big),$$
$$C_{ll'} \triangleq \sum_{l'\neq l}^{L_u}p_{u,l'}\mathbb{E}\Big\{\Big|\sum_{m=1}^{M}\alpha_m\hat{\mathbf{h}}_{ml}^H\mathbf{h}_{ml'}\Big|^2\Big\},$$
$$D_l \triangleq \sum_{k'=1}^{L_d}\mathbb{E}\Big\{\Big|\sum_{m=1}^{M}\sum_{n=1}^{M}\alpha_m\sqrt{\eta_{nk}}\hat{\mathbf{h}}_{ml}^H\mathbf{Q}_{mn}\hat{\mathbf{g}}_{nk}\Big|^2\Big\},$$
$$E_l^u \triangleq \mathbb{E}\Big\{\Big|\sum_{m=1}^{M}\alpha_m\hat{\mathbf{h}}_{ml}^H\Big|^2\Big\}, F_l^u \triangleq \mathbb{E}\Big\{\Big|\sum_{m=1}^{M}\hat{\mathbf{h}}_{ml}^H\tilde{\mathbf{z}}_m\Big|^2\Big\}.$$

Following similar approach as above, the SE of the k-th DL user is expressed by

$$R_k^d = \frac{\tau_s}{\tau_c}\log_2\left(1 + \frac{\varepsilon_k^2|\mathbb{E}\{\sum_{m=1}^{M}\sqrt{\eta_{mk}}\mathbf{g}_{mk}^H\hat{\mathbf{g}}_{mk}\}|^2}{B_k^d + C_{kk'}^d + D_k^d + \tilde{Z}_k^d + \varepsilon_k^2}\right), \quad (5)$$

where B_k^d, $C_{kk'}^d$, and D_k^d denote the BUG, MUI, and UL-to-DL interference at the k-th DL user, respectively; $B_k^d \triangleq \varepsilon_k^2\text{Var}(\sum_{m=1}^{M}\sqrt{\eta_{mk}}\mathbf{g}_{mk}^H\hat{\mathbf{g}}_{mk})$, $D_k^d \triangleq \varepsilon_k^2\sum_{l=1}^{L_u}p_{u,l}\mathbb{E}\{|q_{kl}|^2\}$, and $C_{kk'} \triangleq \varepsilon_k^2\sum_{k'\neq k}^{L_d}\mathbb{E}\{|\sum_{m=1}^{M}\sqrt{\eta_{mk'}}\mathbf{g}_{mk}^H\hat{\mathbf{g}}_{mk'}|^2\}$.

A. Closed-Form Solutions of Spectral Efficiency

To understand the influence of the various system parameters, we rigorously derive the closed-form expressions for the UL/DL SEs in the following Theorems: [6]

[6]Different from [19], where the authors derived the UL rate of HD system by approximating the QN under the assumption of large receive antenna arrays per AP, we derive the exact closed-form solution for the SE under FD settings and further consider the influence of QN at the k-th DL user. Thus our results are valid for arbitrary number of receive antenna arrays thereby aiding the system designer to predict the system performance with high certainty.

Theorem 1: Considering the MRC receiver under imperfect CSI and low-resolution ADCs at the APs, the l-th UL user's achievable SE in the FD CF mMIMO over Rician channels is

$$R_l^u = \frac{\tau_s}{\tau_c}\log_2\left(1 + \frac{p_{u,l}N_{rx}(\sum_{m=1}^{M}\alpha_m a_{ml}^u)^2}{\Upsilon_l^u}\right), \quad (6)$$

where

$$\Upsilon_l^u \triangleq N_{tx}\sum_{k=1}^{L_d}\sum_{m=1}^{M}\sum_{n=1}^{M}\alpha_m^2\eta_{nk}\sigma_{mn}^2 a_{ml}^u a_{nk}^d + \sum_{m=1}^{M}\alpha_m^2 a_{ml}^u + \sum_{l'=1}^{L_u}\sum_{m=1}^{M}p_{u,l'}\alpha_m^2 c_{mll'}^u + \sum_{m=1}^{M}\bar{\alpha}_m\Big(a_{ml}^u + \sum_{l'=1}^{L_u}p_{u,l'}f_{mll'}^u + N_{tx}\sum_{k=1}^{L_d}\sum_{n=1}^{M}\eta_{nk}\sigma_{mn}^2 a_{ml}^u a_{nk}^d\Big),$$

$a_{ml}^u = \zeta_{ml}\bar{\kappa}_{ml}^{-1}(\kappa_{ml}+\mu_{ml})$, $c_{mll'}^u = \zeta_{ml}\zeta_{ml'}\bar{\kappa}_{ml}^{-1}\bar{\kappa}_{ml'}^{-1}(\kappa_{ml} + \kappa_{ml'}\mu_{ml} + \mu_{ml} + \frac{\kappa_{ml}\kappa_{ml'}}{N_{rx}}\phi_{mll'}^2)$, $\bar{\alpha}_m = (\alpha_m - \alpha_m^2)$,
$f_{mll}^u = \zeta_{ml}^2\bar{\kappa}_{ml}^{-2}(\kappa_{ml}^2 + \mu_{ml}^2 + \kappa_{ml} + \mu_{ml} + 3\kappa_{ml}\mu_{ml})$,
$f_{mll'}^u = \zeta_{ml}\zeta_{ml'}\bar{\kappa}_{ml}^{-1}\bar{\kappa}_{ml'}^{-1}(\mu_{ml} + \kappa_{ml} + \kappa_{ml'}\mu_{ml} + \kappa_{ml}\kappa_{ml'})$,

and $\phi_{mll'} = \begin{cases}\frac{\sin(\frac{N_{rx}\pi}{2}\sin(\psi_{mll}^u)-\sin(\psi_{mll'}^u))}{\sin(\frac{\pi}{2}\sin(\psi_{mll}^u)-\sin(\psi_{mll'}^u))}, & \text{for } l'\neq l\\ 0, & \text{for } l'=l.\end{cases}$

Proof: Please refer to Appendix A.

Theorem 2: If the m-th AP employs the MRT precoding over Rician channel and low-resolution ADCs at the k-th DL user, the achievable DL SE in the FD CF mMIMO is written as

$$R_k^d = \frac{\tau_s}{\tau_c}\log_2\left(1 + \frac{\varepsilon_k N_{tx}^2(\sum_{m=1}^{M}\eta_{mk}^{1/2}a_{mk}^d)^2}{\Upsilon_k^d}\right), \quad (7)$$

where $\Upsilon_k^d \triangleq N_{tx}\sum_{k'=1}^{L_d}\sum_{m=1}^{M}c_{mkk'}^d\eta_{mk'} + \sum_{l=1}^{L_u}p_{u,l}\gamma_{kl}^2 + 1 + (1-\varepsilon_k)N_{tx}^2(\sum_{m=1}^{M}\eta_{mk}^{1/2}a_{mk}^d)^2$, $c_{mkk'}^d = \beta_{mk}\beta_{mk'}\bar{\kappa}_{mk}^{-1}\bar{\kappa}_{mk'}^{-1}(\nu_{mk'} + \kappa_{mk'} + \nu_{mk'}\kappa_{mk} + \frac{\kappa_{mk}\kappa_{mk'}\phi_{mkk'}^2}{N_{tx}})$, and

$\phi_{mkk'} = \begin{cases}\frac{\sin(\frac{N_{tx}\pi}{2}\sin(\psi_{mkk}^d)-\sin(\psi_{mkk'}^d))}{\sin(\frac{\pi}{2}\sin(\psi_{mkk}^d)-\sin(\psi_{mkk'}^d))}, & \text{for } k'\neq k\\ 0, & \text{for } k'=k.\end{cases}$

Proof: Please see the Appendix B.

Using (6) and (7), the total sum SE of the FD CF mMIMO with low-resolution ADCs is given by $R_{SE}(\{p_{u,l}\},\{\eta_{mk}\}) = \sum_{l=1}^{L_u}R_l^u + \sum_{k=1}^{L_d}R_k^d$. The sum SE is a function of various parameters including the large-scale fading coefficients, residual SI/IAI, UL-to-DL interference, number of RF chains (i.e., N_{rx}, N_{tx}, and M), UL/DL powers, ADCs resolution b_m^{AP} (and b_k^{UE}).

Remarks: From *Theorem 1*, we observe that the desired signal increases linearly with the AP receive antennas N_{rx} and quadratic in M. The QN grows proportionally with the received signal, i.e., noise, MUI, and residual SI/IAI. Thus, the FD CF mMIMO with low-resolution ADCs is more susceptible to the QN than the HD. Since the desired signal has a higher order (in terms of N_{rx} and M) than the QN, we can compensate for the UL SE loss as a result of the QN, simply

by increasing the RF chains. However, considering *Theorem 2*, it is noted that both the desired signal and QN at the k-th DL user grow at the same rate with N_{tx} and M. Therefore, it is inefficient to compensate for the DL SE due to the QN at the DL users by increasing the transmit antenna arrays. This conclusion is consistent with the Rayleigh fading case [16].

For a fixed DL power, as the UL power increases, the UL SE grows until saturation, i.e., becomes interference-limited while the DL SE decays towards zero since the UL-to-DL interference at the DL users increases with the UL powers. Also, as the DL power increases, for a fixed UL power, the DL SE improves until saturation whereas the UL SE declines towards zero because the residual SI/IAI are enhanced with the increasing DL power. Consider that $p_{u,l} = p_u, \forall l$, $P_{d,m}^{MAX} = P_d^{MAX} = p_d, \forall m$ and $p_u = p_d = p$. Further, let us consider equal power allocation in the DL, i.e., $\eta_{mk} = p\check{\eta}_{mk} N_{tx}^{-1}$, where $\check{\eta}_{mk} = 1/\sum_{k=1}^{L_d} a_{mk}^d$. As $p \to \infty$, the achievable SEs for the l-th UL user and the k-th DL user, respectively, converge to

$$\check{R}_l^u = \frac{\tau_s}{\tau_c} \log_2 \left(1 + \frac{N_{rx} (\sum_{m=1}^{M} \alpha_m a_{ml}^u)^2}{\check{\Upsilon}_l^u} \right), \tag{8}$$

$$\check{R}_k^d = \frac{\tau_s}{\tau_d} \log_2 \left(1 + \frac{\varepsilon_k N_{tx} (\sum_{m=1}^{M} \check{\eta}_{mk}^{1/2} a_{mk}^d)^2}{\check{\Upsilon}_k^d} \right), \tag{9}$$

where $\check{\Upsilon}_l^u \triangleq \sum_{k=1}^{L_d} \sum_{m=1}^{M} \sum_{n=1}^{M} \alpha_m \check{\eta}_{nk} \sigma_{mn}^2 a_{ml}^u a_{nk}^d + \sum_{l'=1}^{L_u} \sum_{m=1}^{M} \alpha_m^2 c_{mll'}^u + \sum_{m=1}^{M} \sum_{l'=1}^{L_u} \bar{\alpha}_m f_{mll'}^u$ and $\check{\Upsilon}_k^d = \sum_{k'=1}^{L_d} \sum_{m=1}^{M} c_{mkk'}^d \check{\eta}_{mk} + \sum_{l=1}^{L_u} \gamma_{kl}^2 + (1 - \varepsilon_k) N_{tx} (\sum_{m=1}^{M} \check{\eta}_{mk} a_{mk}^d)^2$. (8) and (9) demonstrate that the SE loss due to MUI, QN, residual SI/IAI, and UL-to-DL interference cannot be compensated by simply increasing the available transmit powers. Therefore, an efficient power allocation strategy to improve the total sum SE of the FD CF mMIMO with low-resolution ADCs is needed.

To evaluate the impact of the Rician κ-factor, let $\kappa_{mk} = \kappa_{ml} = \kappa, \forall m, k, l$. As $\kappa \to \infty$, the l-th UL and k-th DL users' SEs converge to constants given by (10) and (11), respectively.

$$\bar{R}_l^u = \frac{\tau_s}{\tau_c} \log_2 \left(1 + \frac{p_{u,l} N_{rx} (\sum_{m=1}^{M} \alpha_m \zeta_{ml})^2}{\bar{\Upsilon}_l^u} \right), \tag{10}$$

where $\bar{\Upsilon}_l^u \triangleq N_{tx} \sum_{k=1}^{L_d} \sum_{m=1}^{M} \sum_{n=1}^{M} \alpha_m \zeta_{ml} \sigma_{mn}^2 \eta_{nk} \beta_{nk} + \sum_{l \neq l'}^{L_u} \sum_{m=1}^{M} \frac{p_{u,l'}}{N_{rx}} \alpha_m^2 \zeta_{ml} \zeta_{ml'} \phi_{mll'}^2 + \sum_{m=1}^{M} \alpha_m \zeta_{ml} + \sum_{l'=1}^{L_u} \sum_{m=1}^{M} \bar{\alpha}_m p_{u,l'} \zeta_{ml} \zeta_{ml'}$.

$$\bar{R}_k^d = \frac{\tau_s}{\tau_c} \log_2 \left(1 + \frac{N_{tx}^2 \varepsilon_k (\sum_{m=1}^{M} \eta_{mk}^{1/2} \beta_{mk})^2}{\bar{\Upsilon}_k^d} \right), \tag{11}$$

where $\bar{\Upsilon}_k^d = (1 - \varepsilon_k) N_{tx}^2 (\sum_{m=1}^{M} \beta_{mk} \eta_{mk}^{1/2})^2 + \sum_{l=1}^{L_u} p_{u,l} \gamma_{kl}^2 + \sum_{k' \neq k}^{L_d} \sum_{m=1}^{M} \eta_{mk'} \beta_{mk} \beta_{mk'} \phi_{mkk'}^2 + 1$; $N_{tx} \sum_{k=1}^{L_d} \beta_{mk} \eta_{mk} \leq P_{d,m}^{MAX}$.

Proof: The expressions (10) and (11) are proved by setting the Rician κ-factor in (6) and (7) as κ and taking the limit as $\kappa \to \infty$. From (10) and (11), we note that as the Rician κ-factors increase, the UL/DL SEs saturate irrespective of the channel estimation quality, which is independent of the Rician κ-factor— exposing there exists an SE limit in strong LoS environments.

B. Co-located FD Massive MIMO with Low-Resolution ADCs

For comparison, we derive the SE of the FD co-located mMIMO with low-resolution ADCs. The FD co-located mMIMO is a special case of the FD CF mMIMO, where all the antennas are concentrated at a single BS with $\beta_{mk} = \beta_k$, $\kappa_{mk} = \kappa_k$, $\psi_{mk}^d = \psi_k^d$, $\zeta_{ml} = \zeta_l$, $\kappa_{ml} = \kappa_l$, $\psi_{ml}^u = \psi_l^u$, $\forall m, k, l$ and $\sigma_{AP,mn} = \sigma_{AP}, \forall m$. For simplicity, the BS receive antennas have equal resolution ADCs, i.e., $\alpha_m = \alpha, \forall m$. Corollaries 1 and 2, respectively, provide the UL and DL SEs.

Corollary 1: For the co-located FD mMIMO case, the l-th UL user SE is given by (12) shown at the top of next page. Note that $a_{ml}^u = a_l^u, \forall m$, $f_{mll'}^u = f_{ll'}^u$, $\forall m$, $a_{mk}^d = a_k^d$, $\forall m$, $c_{ll'}^u = \zeta_l \zeta_{l'} \bar{\kappa}_l^{-1} \bar{\kappa}_{l'}^{-1} (\kappa_l + \mu_l + \kappa_{l'} \mu_l + \kappa_l \kappa_{l'} \tilde{\phi}_{ll'}^2 / M N_{rx})$, and $\tilde{\phi}_{ll'} = \begin{cases} \frac{\sin(\frac{M N_{rx} \pi}{2} \sin(\psi_l^u) - \sin(\psi_{l'}^u))}{\sin(\frac{\pi}{2} \sin(\psi_l^u) - \sin(\psi_{l'}^u))}, & \text{for } l' \neq l \\ 0, & \text{for } l' = l. \end{cases}$

Corollary 2: With low-resolution ADCs at the k-th DL user, the k-th DL user SE in the co-located FD mMIMO is written as (13) shown at the top of next page, where $c_{kk'}^d = \beta_k \beta_{k'} \bar{\kappa}_k^{-1} \bar{\kappa}_{k'}^{-1} (\nu_{k'} + \kappa_{k'} + \nu_{k'} \kappa_k + \kappa_k \kappa_{k'} \phi_{kk'}^2 / M N_{tx})$, and $\tilde{\eta}_k = M \eta_{mk}$. Also, we have $\tilde{\phi}_{kk'} = \begin{cases} \frac{\sin(\frac{M N_{tx} \pi}{2} \sin(\psi_k^d) - \sin(\psi_{k'}^d))}{\sin(\frac{\pi}{2} \sin(\psi_k^d) - \sin(\psi_{k'}^d))}, & \text{for } k' \neq k \\ 0, & \text{for } k' = k. \end{cases}$

Proof: The proof is omitted for brevity.

IV. Sum Spectral Efficiency Maximization

In this section, we investigate how to allocate the DL data powers $\{\eta_{mk}\}$ and UL powers $\{p_{u,l}\}$ to maximize the sum SE of the FD CF mMIMO with low-resolution ADCs. First, based on the analytic results from the previous sections, the sum SE optimization problem is formulated. Then, we propose an iterative algorithm via alternating convex optimization.

A. Problem Formulation

The sum SE maximization problem is formulated as

$$\begin{aligned} \underset{\{p_{u,l} \geq 0\}, \{\eta_{mk} \geq 0\}}{\text{Maximize}} \quad & R_{SE}(\{p_{u,l}\}, \{\eta_{mk}\}), \\ \text{subject to} \quad & p_{u,l} \leq P_{u,l}^{MAX}, \ \forall l, \\ & N_{tx} \sum_{k=1}^{L_d} \eta_{mk} a_{mk}^d \leq P_{d,m}^{MAX}, \ \forall m, \end{aligned} \tag{14}$$

where the pre-log factor $\frac{\tau_s}{\tau_c}$ is removed since it does not affect the optimization variables. The first and second constraints indicate that the l-th UL user and m-th AP are limited by their maximum transmit powers $P_{u,l}^{MAX}$ and $P_{d,m}^{MAX}$, respectively.[7] The sum SE maximization problem is a well-known non-convex problem and the global optimum is generally unavailable. Therefore, we exploit the equivalence between the sum SE maximization and the weighted MMSE (WMMSE) minimization problems [35]–[37] to obtain a local optimum. When the WMMSE method is employed in different

[7]The optimization problem does not depend on the instantaneous CSI but only on the large-scale fading coefficients which changes much slowly and thus enables the solution to be used for several coherence intervals.

$$\tilde{R}_l^u = \frac{\tau_s}{\tau_c}\log_2\left(1+\frac{p_{u,l}N_{rx}M\alpha(a_l^u)^2}{a_l^u + N_{tx}M\sum_{k=1}^{L_d}\tilde{\eta}_k\sigma_m^2 a_l^u a_k^d + \sum_{l'=1}^{L_u}p_{u,l'}(\alpha c_{ll'}^u + (1-\alpha)f_{ll'}^u)}\right), \tag{12}$$

$$\tilde{R}_k^d = \frac{\tau_s}{\tau_c}\log_2\left(1+\frac{\varepsilon_k\tilde{\eta}_k(MN_{tx}a_k^d)^2}{(1-\varepsilon_k)\tilde{\eta}_k(MN_{tx}a_k^d)^2 + MN_{tx}\sum_{k'=1}^{L_d}\tilde{\eta}_{k'}c_{kk'}^d + \sum_{l=1}^{L_u}p_{u,l}\gamma_{kl}^2 + 1}\right), \tag{13}$$

systems, the resulting subproblems are unique. Thus, we emphasize that the solutions obtained in this section are novel.

To reformulate problem (14) as WMMSE, we first set $\bar{p}_{u,l} = \sqrt{p_{u,l}}$, $\forall l$ and $\bar{\eta}_{mk} = \sqrt{\eta_{mk}}$, $\forall m,k$. Then, the mean square errors of the l-th UL, i.e., $e_l^u = \mathbb{E}\{|s_l^u - r_l^u\tilde{y}_l^u|^2\}$ and k-th DL users, i.e., $e_k^d = \mathbb{E}\{|s_k^d - r_k^d\tilde{y}_k^d|^2\}$, after detection are written, respectively, as (15) and (16).

$$e_l^u = 1 + |r_l^u|^2 N_{rx}\Big[\sum_{m=1}^{M}\alpha_m a_{ml}^u + \bar{p}_{u,l}^2 N_{rx}(\sum_{m=1}^{M}\alpha_m a_{ml}^u)^2 + \sum_{m=1}^{M}\sum_{l'=1}^{L_u}\bar{p}_{u,l'}^2\alpha_m^2 c_{mll'}^u + N_{tx}\sum_{k=1}^{L_d}\sum_{m=1}^{M}\sum_{n=1}^{M}\alpha_m a_{mk}^d\sigma_{mn}^2 a_{ml}^u\bar{\eta}_{nk}^2 + \sum_{m=1}^{M}\sum_{l'=1}^{L_u}\bar{\alpha}_m\bar{p}_{u,l'}^2 f_{mll'}^u\Big] - 2\bar{p}_{u,l}r_l^u N_{rx}\sum_{m=1}^{M}\alpha_m a_{ml}^u, \tag{15}$$

$$e_k^d = \varepsilon_k|r_k^d|^2\Big[N_{tx}^2(\sum_{m=1}^{M}a_{mk}^d\bar{\eta}_{mk})^2 + N_{tx}\sum_{k'=1}^{L_d}\sum_{m=1}^{M}c_{mkk'}^d\bar{\eta}_{mk'}^2 + \sum_{l=1}^{L_u}\bar{p}_{u,l}^2\gamma_{kl}^2 + 1\Big] + 1 - 2\varepsilon_k r_k^d N_{tx}\sum_{m=1}^{M}a_{mk}^d\bar{\eta}_{mk}, \tag{16}$$

where r_l^u and r_k^d (newly introduced optimization variables) are the l-th UL and k-th DL users receive filters, respectively.

Proof: The proof follows similar approach as Appendix A.

Subsequently, the WMMSE problem is formulated as

$$\begin{aligned}\underset{\substack{\{\bar{p}_{u,l}\geq 0\},\{\omega_l^u\geq 0\},\{r_l^u\},\\ \{\bar{\eta}_{mk}\geq 0\},\{\omega_k^d\geq 0\},\{r_k^d\}}}{\text{Minimize}} \quad & \Gamma(\{\omega_l^u, r_l^u, \bar{p}_{u,l}\},\{\omega_k^d, r_k^d, \bar{\eta}_{mk}\}) \\ \text{subject to} \quad & \bar{p}_{u,l}^2 \leq P_{u,l}^{MAX}, \ \ \forall l, \\ & N_{tx}\sum_{k=1}^{L_d}\bar{\eta}_{mk}^2 a_{mk}^d \leq P_{d,m}^{MAX}, \forall m, \end{aligned} \tag{17}$$

where $\Gamma(\{\omega_l^u, r_l^u, \bar{p}_{u,l}\},\{\omega_k^d, r_k^d, \bar{\eta}_{mk}\}) \triangleq \sum_{l=1}^{L_u}[\omega_l^u e_l^u - \ln(\omega_l^u)] + \sum_{k=1}^{L_d}[\omega_k^d e_k^d - \ln(\omega_k^d)]$; ω_l^u and ω_k^d denote the positive weights associated with the l-th UL user and the k-th DL user, respectively, for the WMMSE equivalent problem.[8]

B. Iterative Algorithm

Here, we develop an iterative algorithm based on the alternating convex optimization, where one variable is optimized while the others are fixed. For constant $\{\omega_l^u\}$, $\{\bar{p}_{u,l}\}$, $\{\omega_k^d\}$, $\{r_k^d\}$, and $\{\bar{\eta}_{mk}\}$, the optimal r_l^u that minimizes the objective function of (17) is achieved by taking the first-order derivative with respect to (wrt) r_l^u, equating to zero and solving for r_l^u. Thus, we have

$$r_l^u\Big[\bar{p}_{u,l}^2 N_{rx}(\sum_{m=1}^{M}\alpha_m a_{ml}^u)^2 + \sum_{l'=1}^{L_u}\sum_{m=1}^{M}\alpha_m^2\bar{p}_{u,l'}^2 c_{mll'}^u + \sum_{m=1}^{M}\alpha_m a_{ml}^u + N_{tx}\sum_{k=1}^{L_d}\sum_{m=1}^{M}\sum_{n=1}^{M}\alpha_m a_{mk}^d\sigma_{mn}^2 a_{ml}^u\bar{\eta}_{nk}^2 + \sum_{l'=1}^{L_u}\sum_{m=1}^{M}\bar{\alpha}_m\bar{p}_{u,l'}^2 f_{mll'}^u\Big] - \bar{p}_{u,l}\sum_{m=1}^{M}\alpha_m a_{ml}^u = 0. \tag{18}$$

From (18), the optimal filter $r_l^{u\star}$ of the l-th UL user is $r_l^{u\star} = \bar{p}_{u,l}\sum_{m=1}^{M}\alpha_m a_{ml}^u(\tilde{r}_l^u)^{-1}$, where

$$\tilde{r}_l^u \triangleq \bar{p}_{u,l}^2 N_{rx}(\sum_{m=1}^{M}\alpha_m a_{ml}^u)^2 + \sum_{l'=1}^{L_u}\sum_{m=1}^{M}\alpha_m^2\bar{p}_{u,l'}^2 c_{mll'}^u + N_{tx}\sum_{k=1}^{L_d}\sum_{m=1}^{M}\sum_{n=1}^{M}\alpha_m a_{mk}^d\sigma_{mn}^2 a_{ml}^u\bar{\eta}_{nk}^2 + \sum_{m=1}^{M}\alpha_m a_{ml}^u + \sum_{l'=1}^{L_u}\sum_{m=1}^{M}\bar{\alpha}_m\bar{p}_{u,l'}^2 f_{mll'}^u.$$

Next, we derive the l-th UL user weight that minimizes the objective function of (17) by keeping $\{r_l^u\}$, $\{r_k^d\}$, $\{\omega_k^d\}$, $\{\bar{p}_{u,l}\}$, and $\{\bar{\eta}_{mk}\}$ constant, solving the first-order derivative wrt ω_l^u, setting the gradient to zero and solving for ω_l^u. Thus, the optimal weight $\omega_l^{u\star} = (e_l^u)^{-1}$ is attained.

Using similar approach, the k-th DL user's optimal filter is expressed as $r_k^{d\star} = N_{tx}\sum_{m=1}^{M}a_{mk}^d\bar{\eta}_{mk}(\tilde{r}_k^d)^{-1}$, where $\tilde{r}_k^d = 1 + N_{tx}^2(\sum_{m=1}^{M}a_{mk}^d\bar{\eta}_{mk})^2 + N_{tx}\sum_{k'=1}^{L_d}\sum_{m=1}^{M}c_{mkk'}^d\bar{\eta}_{mk'}^2 + \sum_{l=1}^{L_u}\gamma_{kl}^2\bar{p}_{u,l}^2$. The optimal weight of the k-th DL user is given by $\omega_k^{d\star} = (e_k^d)^{-1}$.

For a given set of variables $\{\omega_l^u\}$, $\{r_l^u\}$, $\{\omega_k^d\}$, and $\{r_k^d\}$, we now need to solve for the optimal data powers $\{\bar{p}_{u,l}\}$ and $\{\bar{\eta}_{mk}\}$ that minimize the objective function. Expanding the objective function of (17), grouping like terms and removing known terms, the problem (17) reduces to

$$\begin{aligned}\underset{\{\bar{p}_{u,l}\geq 0\},\{\bar{\eta}_{mk}\geq 0\},}{\text{Minimize}} \quad & \bar{\Gamma}_u(\{\bar{p}_{u,l}\}) + \bar{\Gamma}_d(\{\bar{\eta}_{mk}\}) \\ \text{subject to} \quad & \bar{p}_{u,l}^2 \leq P_{u,l}^{MAX}, \ \ \forall l, \\ & N_{tx}\sum_{k=1}^{L_d}\bar{\eta}_{mk}^2 a_{mk}^d \leq P_{d,m}^{MAX}, \ \forall m, \end{aligned} \tag{19}$$

[8]The WMMSE problem is concave, and the global optimum can be achieved. Its convexity can be proved from the second derivative of the objective function. However, this is straightforward to establish and is omitted from the paper for brevity.

where

$$\bar{\Gamma}_u(\{\bar{p}_{u,l}\}) = \sum_{l=1}^{L_u} \omega_l^u |r_l^u|^2 N_{rx} \Big[\bar{p}_{u,l}^2 N_{rx} (\sum_{m=1}^{M} \alpha_m a_{ml}^u)^2 + \sum_{m=1}^{M} \sum_{l'=1}^{L_u} \bar{p}_{u,l'}^2 \alpha_m^2 c_{mll'}^u + \sum_{l'=1}^{L_u} \sum_{m=1}^{M} \bar{\alpha}_m \bar{p}_{u,l'}^2 f_{mll'}^u \Big] - 2 \sum_{l=1}^{L_u} \omega_l^u \times \bar{p}_{u,l} r_l^u N_{rx} \sum_{m=1}^{M} \alpha_m a_{ml}^u + \sum_{k=1}^{L_d} \omega_k^d |r_k^d|^2 \sum_{l=1}^{L_u} \gamma_{kl}^2 \bar{p}_{u,l}^2,$$

$$\bar{\Gamma}_d(\{\bar{\eta}_{mk}\}) = \sum_{k=1}^{L_d} \omega_k^d |r_k^d|^2 \varepsilon_k \Big[N_{tx}^2 (\sum_{m=1}^{M} a_{mk}^d \bar{\eta}_{mk})^2 + N_{tx} \sum_{k'=1}^{L_d} \sum_{m=1}^{M} c_{mkk'}^d \bar{\eta}_{mk'}^2 \Big] - 2 \sum_{k=1}^{L_d} \omega_k^d \varepsilon_k r_k^d N_{tx} \sum_{m=1}^{M} a_{mk}^d \bar{\eta}_{mk} + \sum_{l=1}^{L_u} \omega_l^u |r_l^u|^2 N_{rx} N_{tx} \sum_{k=1}^{L_d} \sum_{m=1}^{M} \sum_{n=1}^{M} \alpha_m a_{mk}^d \sigma_{mn}^2 a_{ml}^u \bar{\eta}_{nk}^2.$$

It is noted that the problem (19) can be decomposed and the power allocation problem at the UL users and the APs can be solved separately. Considering the UL, we obtain

$$\underset{\{\bar{p}_{u,l} \geq 0\},}{\text{Minimize}} \quad \bar{\Gamma}_u(\{\bar{p}_{u,l}\}), \text{subject to } \bar{p}_{u,l}^2 \leq P_{u,l}^{MAX}, \forall l, \quad (20)$$

while for the DL, i.e., AP power allocation problem, we have

$$\begin{aligned} \underset{\{\bar{\eta}_{mk} \geq 0\},}{\text{Minimize}} \quad & \bar{\Gamma}_d(\{\bar{\eta}_{mk}\}), \\ \text{subject to} \quad & N_{tx} \sum_{k=1}^{L_d} \bar{\eta}_{mk}^2 a_{mk}^d \leq P_{d,m}^{MAX}, \forall m. \end{aligned} \quad (21)$$

1) Solving UL User Power Control Problem (20)*:* The problem (20) is a convex quadratic program wrt $\bar{p}_{u,l}$ and therefore its optimal solution can easily be achieved in closed-form by using the Lagrange multiplier method. Specifically, the Lagrangian of the problem (20) is written as

$$\mathcal{L}(\{\lambda_l\}, \{\bar{p}_{u,l}\}) = \bar{\Gamma}_u(\{\bar{p}_{u,l}\}) + \sum_{l=1}^{L_u} \lambda_l (\bar{p}_{u,l}^2 - P_{u,l}^{MAX}), \quad (22)$$

where $\lambda_l \geq 0$ is the Lagrange multiplier. By taking the first derivative of (22) wrt $\bar{p}_{u,l}$, we have

$$\frac{\partial \mathcal{L}}{\partial \bar{p}_{u,l}} = 2\bar{p}_{u,l} N_{rx}^2 \omega_l^u |r_l^u|^2 (\sum_{m=1}^{M} \alpha_m a_{ml}^u)^2 + 2\bar{p}_{u,l} N_{rx} \times \sum_{l'=1}^{L_u} \sum_{m=1}^{M} \omega_{l'}^u |r_{l'}^u|^2 \alpha_m^2 c_{mll'}^u - r_l^u \omega_l^u N_{rx} \sum_{m=1}^{M} \alpha_m a_{ml}^u + 2\bar{p}_{u,l} N_{rx} \sum_{l'=1}^{L_u} \sum_{m=1}^{M} \omega_{l'}^u |r_{l'}^u|^2 \bar{\alpha}_m f_{mll'}^u + 2\bar{p}_{u,l} \sum_{k=1}^{L_d} \omega_k^d |r_k^d|^2 \gamma_{kl}^2 + 2\bar{p}_{u,l} \lambda_l.$$

Equating the derivative to zero and solving for $\bar{p}_{u,l}$, we obtain $\bar{p}_{u,l} = r_l^u \omega_l^u N_{rx} \sum_{m=1}^{M} \alpha_m a_{ml}^u / (\psi_{u,l} + \lambda_l)$, where

$$\psi_{u,l} = N_{rx}^2 \omega_l^u |r_l^u|^2 (\sum_{m=1}^{M} \alpha_m a_{ml}^u)^2 + \sum_{k=1}^{L_d} \omega_k^d |r_k^d|^2 \gamma_{kl}^2 + N_{rx} \times \sum_{l'=1}^{L_u} \sum_{m=1}^{M} \omega_{l'}^u |r_{l'}^u|^2 \alpha_m^2 c_{mll'}^u + N_{rx} \sum_{l'=1}^{L_u} \sum_{m=1}^{M} \omega_{l'}^u |r_{l'}^u|^2 \bar{\alpha}_m f_{mll'}^u.$$

The Lagrange multiplier λ_l has to satisfy the complementary slackness condition [36], i.e., $\lambda_l (\bar{p}_{u,l}^2 - P_u^{MAX}) = 0$. Therefore, the solution of $\bar{p}_{u,l}$ is

$$\bar{p}_{u,l} = \begin{cases} \min(\hat{p}_{u,l}, \sqrt{P_{u,l}^{MAX}}), & \text{for } \lambda_l = 0 \\ \sqrt{P_{u,l}^{MAX}}, & \text{for } \lambda_l \neq 0, \end{cases} \quad (23)$$

where $\hat{p}_{u,l} = r_l^u \omega_l^u N_{rx} \sum_{m=1}^{M} \alpha_m a_{ml}^u (\psi_{u,l})^{-1}$.

2) Solving DL Power Allocation Problem (21)*:* The problem (21) is a quadratic constraint quadratic program hence convex optimization problem. However, the optimization variables in the objective function are coupled together via the per AP power constraints. To decouple the problem, we leverage the alternating direction method of multipliers (ADMM) [38]. Let $\bar{\boldsymbol{\eta}}_k = [\bar{\eta}_{1k}, \cdots, \bar{\eta}_{Mk}] \in \mathbb{R}^{M \times 1}$, $\bar{\boldsymbol{\eta}} = [\bar{\boldsymbol{\eta}}_1^T, \cdots, \bar{\boldsymbol{\eta}}_{L_d}^T]^T \in \mathbb{R}^{ML_d \times 1}$, $\mathbf{a}_k^d = [a_{1k}^d, \cdots, a_{Mk}^d]^T \in \mathbb{R}^{M \times 1}$, $\mathbf{c}_{kk'}^d = [c_{1kk'}^d, c_{2kk'}^d, \cdots, c_{Mkk'}^d] \in \mathbb{R}^{M \times 1}$, $\mathbf{C}_{kk'}^d = \text{diag}(\mathbf{c}_{kk'}^d) \in \mathbb{R}^{M \times M}$, and $\mathbf{D}_k^d = \text{diag}\Big(\sum_{l=1}^{L_u} \sum_{m=1}^{M} \omega_l^u |r_l^u|^2 \alpha_m a_{ml}^u \sigma_{m1}^2 a_{1k}^d, \cdots, \sum_{l=1}^{L_u} \sum_{m=1}^{M} \omega_l^u |r_l^u|^2 \alpha_m a_{ml}^u \sigma_{mM}^2 a_{Mk}^d \Big) \in \mathbb{R}^{M \times M}$. Therefore, the objective function of (21) is rewritten by

$$\bar{\Gamma}_d(\bar{\boldsymbol{\eta}}) = N_{tx} \Big[\sum_{k=1}^{L_d} \omega_k^d |r_k^d|^2 \varepsilon_k \Big(N_{tx} |\bar{\boldsymbol{\eta}}_k^T \mathbf{a}_k^d|^2 + \sum_{k'=1}^{L_d} \bar{\boldsymbol{\eta}}_{k'}^T \mathbf{C}_{kk'}^d \bar{\boldsymbol{\eta}}_{k'} \Big) - 2 \sum_{k=1}^{L_d} \omega_k^d \varepsilon_k r_k^d |\bar{\boldsymbol{\eta}}_k^T \mathbf{a}_k^d| + N_{rx} \sum_{k=1}^{L_d} \bar{\boldsymbol{\eta}}_k^T \mathbf{D}_k^d \bar{\boldsymbol{\eta}}_k \Big].$$

Also, let $\mathcal{F}$ define the feasible region of the constraint in (21) and $g_{\mathcal{F}}(\mathbf{z})$ as an indicator function which is given by

$$g_{\mathcal{F}}(\mathbf{z}) = \begin{cases} 0, & \text{if } N_{tx} \sum_{k=1}^{L_d} z_{mk}^2 a_{mk}^d \leq p_{d,m}^{MAX} \\ +\infty, & \text{otherwise} \end{cases}.$$

where $\mathbf{z} = [\mathbf{z}_1^T, \cdots, \mathbf{z}_{L_d}^T] \in \mathbb{R}^{ML_d \times 1}$ and $\mathbf{z}_k = [z_{1k}, \cdots, z_{Mk}]^T \in \mathbb{R}^{M \times 1}$. The optimization problem (21) is recast in ADMM form as [38]

$$\underset{\bar{\boldsymbol{\eta}}, \mathbf{z}}{\text{Minimize}} \quad \bar{\Gamma}_d(\bar{\boldsymbol{\eta}}) + g_{\mathcal{F}}(\mathbf{z}), \text{ subject to } \quad \bar{\boldsymbol{\eta}} = \mathbf{z}. \quad (24)$$

The scaled form augmented Lagrangian is written by [38]

$$\mathcal{L}_\varrho(\bar{\boldsymbol{\eta}}, \mathbf{z}, \mathbf{u}) = \bar{\Gamma}(\bar{\boldsymbol{\eta}}) + g_{\mathcal{F}}(\mathbf{z}) + \frac{\varrho}{2} \sum_{k=1}^{L_d} \|\bar{\boldsymbol{\eta}}_k - \mathbf{z}_k + \mathbf{u}_k\|^2,$$

where $\varrho > 0$ and $\mathbf{u} = [\mathbf{u}_1^T, \cdots, \mathbf{u}_{L_d}^T] \in \mathbb{R}^{ML_d \times 1}$ denote the penalty parameter and scaled dual variable, respectively; $\mathbf{u}_k = [u_{1k}, u_{2k}, \cdots, u_{Mk}]^T \in \mathbb{R}^{M \times 1}$. The ADMM for minimizing the augmented Lagrangian $\mathcal{L}_\varrho(\bar{\boldsymbol{\eta}}, \mathbf{z}, \mathbf{u})$ is carried

Algorithm 1 ADMM Technique for Finding Solution to (21)

Input: Initialize the primal variables $z_{mk}^{(0)}, \forall m,k$ and the dual variable $u_{mk}^{(0)}, \forall m,k$ and set the penalty $\varrho > 0$. Set $s = 1$.

1. Iteration s:

1.1. Update the first primal variables as

$$\bar{\boldsymbol{\eta}}^s := \underset{\bar{\boldsymbol{\eta}}}{\text{argmin}} \ \mathcal{L}_\varrho(\bar{\boldsymbol{\eta}}, \mathbf{z}^{s-1}, \mathbf{u}^{s-1}). \tag{25}$$

1.2. Update the second primal variables $\mathbf{z}_m^{(s)}, \forall m$ as

$$\mathbf{z}^s := \underset{\mathbf{z}}{\text{argmin}} \ \mathcal{L}_\varrho(\bar{\boldsymbol{\eta}}^s, \mathbf{z}, \mathbf{u}^{s-1}). \tag{26}$$

1.3. Update the dual variables $\mathbf{u}$

$$\mathbf{u}^s := \mathbf{u}^{s-1} + \bar{\boldsymbol{\eta}}^s - \mathbf{z}^s. \tag{27}$$

2. If stopping criteria is met $\rightarrow$ Stop. Else go to Step 3.
3. Store the current best solution $\bar{\eta}_{mk}^{(s)}$, $z_{mk}^{(s)}$, and $u_{mk}^{(s)}$, $\forall m,k$. Set $s = s+1$ and go to Step 1.

Output: The optimal solution: $\bar{\eta}_{mk}^\star = \bar{\eta}_{mk}^{(s)}, \forall m,k$.

out by alternatively updating the two blocks of primal variables $\bar{\boldsymbol{\eta}}$ and $\mathbf{z}$ as summarized by Algorithm 1.

Below, we will detail the procedure to update $\bar{\boldsymbol{\eta}}$ and $\mathbf{z}$ with closed-form expressions. For ease of notation, we omit the superscripts that represent the iteration counter. The first block of primal update in (25) is obtained by solving the unconstrained convex quadratic problem given by

$$\underset{\bar{\boldsymbol{\eta}}}{\text{Minimize}} \quad \bar{\Gamma}_d(\bar{\boldsymbol{\eta}}) + \frac{\varrho}{2}\sum_{k=1}^{L_d}\|\bar{\boldsymbol{\eta}}_k - \mathbf{z}_k + \mathbf{u}_k\|^2. \tag{28}$$

The objective function of (28) is expanded as

$$\sum_{k=1}^{L_d}\bar{\boldsymbol{\eta}}_k^T\Big(\omega_k^d|r_k^d|^2\varepsilon_k N_{tx}^2\mathbf{a}_k^d(\mathbf{a}_k^d)^T + N_{tx}\sum_{k'=1}^{L_d}\omega_{k'}^d|r_{k'}^d|^2\varepsilon_k\mathbf{C}_{kk'} + N_{rx}N_{tx}\mathbf{D}_k + \frac{\varrho}{2}\mathbf{I}_M\Big)\bar{\boldsymbol{\eta}}_k - 2\sum_{k=1}^{L_d}\boldsymbol{\eta}_k^T\Big(\omega_k\varepsilon_k r_k^d N_{tx}\mathbf{a}_k^d + \frac{\varrho}{2}(\mathbf{z}_k - \mathbf{u}_k)\Big) + \frac{\varrho}{2}\sum_{k=1}^{L_d}(\mathbf{z}_k^T\mathbf{z}_k + \mathbf{u}_k^T\mathbf{u}_k - 2\mathbf{z}_k^T\mathbf{u}_k). \tag{29}$$

The optimal $\bar{\boldsymbol{\eta}}_k^\star, \forall k$ is achieved by setting the first derivative of (29) wrt $\bar{\boldsymbol{\eta}}_k$ to zero and solving for $\bar{\boldsymbol{\eta}}_k$. Thus, we have

$$\bar{\boldsymbol{\eta}}_k^\star = \mathbf{W}_k^{-1}(\omega_k\varepsilon_k r_k^d N_{tx}\mathbf{a}_k^d + \frac{\varrho}{2}(\mathbf{z}_k - \mathbf{u}_k)), \ \ \forall k, \tag{30}$$

where $\mathbf{W}_k \triangleq \omega_k^d|r_k^d|^2\varepsilon_k N_{tx}^2\mathbf{a}_k^d(\mathbf{a}_k^d)^T + N_{tx}\sum_{k'=1}^{L_d}\omega_{k'}^d|r_{k'}^d|^2\varepsilon_k\mathbf{C}_{kk'}^d + N_{rx}N_{tx}\mathbf{D}_k^d + \frac{\varrho}{2}\mathbf{I}_M$.

Next, the second block of primal variables $\mathbf{z}$ are updated by solving the optimization problem

$$\begin{aligned}\underset{\mathbf{z}}{\text{Minimize}} \quad & \frac{\varrho}{2}\sum_{k=1}^{L_d}\|\bar{\boldsymbol{\eta}}_k - \mathbf{z}_k + \mathbf{u}_k\|^2, \\ \text{subject to} \quad & N_{tx}\sum_{k=1}^{L_d} z_{mk}^2 a_{mk}^d \le P_{d,m}^{MAX}, \forall m.\end{aligned} \tag{31}$$

From observation, the problem (31) can be separated into M subproblems with the m-th subproblem corresponding to the m-th AP. Specifically, $\forall m = 1,\cdots,M$, we have

$$\begin{aligned}\underset{\mathbf{z}_m}{\text{Minimize}} \quad & \frac{\varrho}{2}\sum_{k=1}^{L_d}(\bar{\eta}_{mk} - z_{mk} + u_{mk})^2, \\ \text{subject to} \quad & N_{tx}\sum_{k=1}^{L_d} z_{mk}^2 a_{mk}^d \le P_{d,m}^{MAX},\end{aligned} \tag{32}$$

where $\mathbf{z}_m = [z_{m1},\cdots,z_{mL_d}]^T \in \mathbb{R}^{L_d\times 1}$, $\bar{\boldsymbol{\eta}}_m = [\bar{\eta}_{m1},\cdots,\bar{\eta}_{mL_d}]^T \in \mathbb{R}^{L_d\times 1}$, $\mathbf{u}_m = [u_{m1},\cdots,u_{mL_d}]^T \in \mathbb{R}^{L_d\times 1}$, and $\bar{\mathbf{a}}_m^d = [\sqrt{a_{m1}^d},\cdots,\sqrt{a_{mL_d}^d}]^T \in \mathbb{R}^{L_d\times 1}$. Problem (31) is rewritten as

$$\begin{aligned}\underset{\mathbf{z}_m}{\text{Minimize}} \quad & \|\bar{\boldsymbol{\eta}}_m - \mathbf{z}_m + \mathbf{u}_m\|^2, \\ \text{subject to} \quad & N_{tx}\|\mathbf{z}_m^T\bar{\mathbf{a}}_m^d\|^2 \le P_{d,m}^{MAX},\end{aligned} \tag{33}$$

The optimal solution to (33) is obtained by using the KKT conditions. Thus, for each subproblem, we have the solution $\mathbf{z}_m^\star = \min\Big(1, \sqrt{p_{d,m}^{MAX}/N_{tx}\|\bar{\mathbf{a}}_m^d\|^2\|\boldsymbol{\xi}_m\|^2}\Big)\boldsymbol{\xi}_m$, $\forall m = 1,\cdots,M$, where $\boldsymbol{\xi}_m = \bar{\boldsymbol{\eta}}_m + \mathbf{u}_m$. The dual variable $\mathbf{u}$ updates are done by a simple addition of the two primal variables.

Until now, the closed-form expressions for the variable updates have been derived. In terms of computational complexity, the only expensive process is the matrix inversion in (30). However, this computation is carried out once for any large-scale fading realization. The primal variables $z_{mk}, \forall m,k$ in Algorithm 1 can be initialized to any values within the feasible region. In this paper, $z_{mk}, \forall m,k$ is initialized as $z_{mk} = \bar{\eta}_{mk}, \forall m,k$ and the dual variables are initialized by $u_{mk} = 0, \forall m,k$. The ADMM algorithm is guaranteed to converge to a global optimum as noted in [38] and references therein. The stopping criteria which is proposed by [38] is used to terminate Algorithm 1, where the $\epsilon^{rel} = 10^{-3}$. Finally, the iterative algorithm based on the alternating optimization technique for finding solution to (14) is summarized in Algorithm 2. Algorithm 2 is initialized with any data power values in the feasible set and it is terminated when the difference between two successive iterations (i.e., $\vartheta \ge 0$) is small. We define a stopping criterion for Algorithm 2 as $|R_{SE}^{(t)} - R_{SE}^{(t-1)}| \le \vartheta$.

3) Computational Complexity: The complexity for implementing Algorithms 1 and 2 are $\mathcal{O}(I_1[M^3L_d^3 + \log(1+\phi_1)])$ and $\mathcal{O}(I_2\{I_1[M^3L_d^3 + \log(1+\phi_1)] + L_u^5L_d^5 + \log(1+\phi_2)\})$, respectively. Note that Algorithm 1 is embedded in Algorithm 2. Here, $\log(1+\phi_1)$ and $\log(1+\phi_2)$ represent the complexity for implementing the convergence criteria of Algorithms 1 and 2, respectively. The computation of variables $\bar{\boldsymbol{\eta}}$, $\mathbf{z}^s$ and $\mathbf{u}^s$ in Algorithm 1 is $M^3L_d^3$. The computation of $\{\bar{p}_{u,l}\}_{l=1}^{L_u}$, $\{r_l^u\}_{l=1}^{L_u}$, $\{\omega_l^u\}_{l=1}^{L_u}$, $\{e_l^u\}_{l=1}^{L_u}$, $\{r_k^d\}_{k=1}^{L_d}$, $\{\omega_k^d\}_{k=1}^{L_d}$, $\{e_k^d\}_{k=1}^{L_d}$, and the sum SE is given as $L_u^5L_d^4$. The computation of the iterations within

Algorithm 2 Alternating Optimization for (17)

Input: Maximum data powers per UL user $P_{u,l}^{MAX}$ and AP P_m^{MAX}. Initialize powers $\bar{p}_{u,l}^{(0)}, \forall l$ and $\bar{\eta}_{mk}^{(0)}, \forall m,k$. Set $t=1$.

1. Iteration t:
   - 1.1. Update $r_l^{u(t)}, \forall l$ as $r_l^{u(t)} = \frac{\bar{p}_{u,l}^{(t-1)} \sum_{m=1}^{M} \alpha_m a_{ml}^u}{\tilde{r}_l^{u(t-1)}}$ where $\tilde{r}_l^{u(t-1)}$ is written as (34).
   - 1.2. Update $\omega_l^{u(t)}, \forall l$ as $\omega_l^{u(t)} = \left(e_l^{u(t)}\right)^{-1}$, where $e_l^{u(t)} = 1 - 2N_{rx} r_l^{u(t)} \bar{p}_{u,l}^{(t-1)} \sum_{m=1}^{M} \alpha_m a_{ml}^u + |r_l^{u(t)}|^2 N_{rx} \tilde{r}_l^{u(t-1)}$.
   - 1.3. Update $r_k^{d(t)}, \forall k$ as $r_k^{d(t)} = \frac{N_{tx} \sum_{m=1}^{M} a_{mk}^d \bar{\eta}_{mk}^{(t-1)}}{\tilde{r}_k^{d(t-1)}}$, where $\tilde{r}_k^{d(t-1)}$ is given by (35).
   - 1.4. Update the variables $\omega_k^{d(t)}, \forall k$ as $\omega_k^{d(t)} = \left(e_k^{d(t)}\right)^{-1}$, where $e_k^{d(t)} = 1 - 2\varepsilon_k r_k^{d(t)} N_{tx} \sum_{m=1}^{M} a_{mk}^d \bar{\eta}_{mk}^{(t-1)} + |r_k^{d(t)}|^2 \varepsilon_k \tilde{r}_k^{d(t-1)}$.
   - 1.5. Update $\bar{p}_{u,l}^{(t)}, \forall l$ as $\bar{p}_{u,l}^{(t)} = \min\left(\hat{p}_{u,l}, \sqrt{P_{u,l}^{MAX}}\right)$, where $\hat{p}_{u,l}$ is given by (36).
   - 1.6. Update $\bar{\eta}_{mk}^{(t)}, \forall m,k$ using Algorithm 1 with the inputs $\{r_l^{u(t)}, \omega_l^{u(t)}\}$, and $\{r_k^{d(t)}, \omega_k^{d(t)}\}$.
2. If stopping criterion is met $\rightarrow$ Stop. Else go to Step 3.
3. Save the current solution, i.e., $\bar{p}_{u,l}^{(t)}, \forall l$ and $\bar{\eta}_{mk}^{(t)}, \forall m,k$. Set $t = t+1$ and go to Step 1.

Output: The optimal solutions: $\bar{p}_{u,l}^{(t)}, \forall l$ and $\bar{\eta}_{m,k}^{(t)}, \forall m,k$.

Algorithms 1 and 2 are defined as I_1 and I_2, respectively.

$$\tilde{r}_l^{u(t-1)} = \sum_{m=1}^{M} \alpha_m a_{ml}^u + (\bar{p}_{u,l}^{(t-1)})^2 N_{rx} \Big(\sum_{m=1}^{M} \alpha_m a_{ml}^u \Big)^2 + \sum_{l'=1}^{L_u} \sum_{m=1}^{M} (\bar{p}_{u,l'}^{(t-1)})^2 (\alpha_m^2 c_{mll'}^u + \bar{\alpha}_m f_{mll'}^u) + N_{tx} \sum_{k=1}^{L_d} \sum_{m=1}^{M} \sum_{n=1}^{M} \alpha_m a_{mk}^d \sigma_{mn}^2 a_{ml}^u (\bar{\eta}_{nk}^{(t-1)})^2. \quad (34)$$

$$\tilde{r}_k^{d(t-1)} = 1 + \sum_{l=1}^{L_u} \gamma_{kl}^2 (\bar{p}_{u,l}^{(t-1)})^2 + N_{tx}^2 \Big(\sum_{m=1}^{M} a_{mk}^d \bar{\eta}_{mk}^{(t-1)} \Big)^2 + N_{tx} \sum_{k'=1}^{L_d} \sum_{m=1}^{M} c_{mkk'}^d (\bar{\eta}_{mk'}^{(t-1)})^2. \quad (35)$$

$$\hat{p}_{ul} = r_l^{u(t)} \omega_l^{u(t)} N_{rx} \sum_{m=1}^{M} \alpha_m a_{ml}^u \Big(N_{rx}^2 \omega_l^{u(t)} |r_l^{u(t)}|^2 \times \Big(\sum_{m=1}^{M} \alpha_m a_{ml}^u \Big)^2 + N_{rx} \sum_{l'=1}^{L_u} \sum_{m=1}^{M} \omega_{l'}^{u(t)} |r_{l'}^{u(t)}|^2 (\alpha_m^2 c_{mll'}^u + \bar{\alpha}_m f_{mll'}^u) + \sum_{k=1}^{L_d} \omega_k^{d(t)} |r_k^{d(t)}|^2 \gamma_{kl}^2 \Big)^{-1}. \quad (36)$$

V. Numerical Results

This section presents results of the paper. Analytic results are validated through Monte Carlo simulations over 500 channel realizations and 10^3 AP-user random locations. The M APs, L_u UL, and L_d DL users are uniformly distributed within a 1 km^2 cell which is wrapped-around at the edges similar to [3]. The large-scale fading coefficient between any two nodes i and j is given by $10^{PL_{ij}}$, where PL_{ij} is the pathloss. The pathloss between the m-th AP and the k-th DL user (l-th UL user) is calculated using the COST 231 Walfish-Ikegami model for micro-cells, where the AP height is 12.5 m with the user height 1.5 m and an LoS exists between any AP-user link. Specifically, the AP-user pathloss is written as $PL_{ij} = -30.18 - 26\log_{10}(d_{ij}) + S_{ij}$, where S_{ij} is the lognormal shadow fading with the standard deviation 4 dB and d_{ij} is the distance between nodes i and j in meters [39]. For the inter-AP and UL-to-DL user pathloss, we use the COST 231 Walfish-Ikegami model for non-LoS which is expressed as $PL_{ij} = -34.53 - 38\log_{10}(d_{ij})$. The Rician κ-factor κ_{ij} is computed as $\kappa_{ij} = 10^{1.3-0.003 d_{ij}}$ [39].

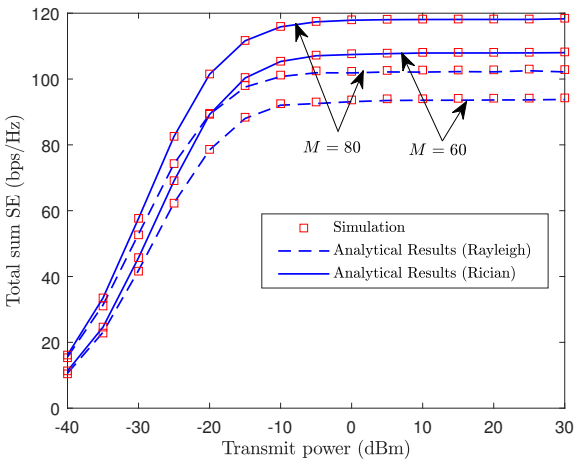

Fig. 2: Total sum SE vs power (dBm) ($L_u = L_d = 20$, $b_m^{AP} = b_k^{UE} = 3$, $N_{rx} = N_{tx} = 5$).

Communication occurs over 20 MHz bandwidth with a total receiver noise power $N_o = -94$ dBm. Each coherence interval comprises $\tau_c = 200$, where $\tau_u = L_u$ and $\tau_d = L_d$. Also, $p_\tau = \tilde{p}_\tau / N_o$, $P_{d,m}^{MAX} = \tilde{P}_{d,m}^{MAX}/N_o$, and $P_{u,l}^{MAX} = \tilde{P}_{u,l}^{MAX}/N_o$, where $\tilde{p}_\tau$, $\tilde{P}_{d,m}^{MAX}$, and $\tilde{P}_{u,l}^{MAX}$ is the pilot power, maximum powers available per AP and UL user, respectively. For simplicity, we assume all the APs use equal resolution ADCs, i.e., $b_m^{AP} = b^{AP}, \forall m$. Similar settings are made for the DL users, i.e., $b_k^{UE} = b^{UE}, \forall k$. To obtain α_m and ε_k for any b_k^{UE} and b_m^{AP}, see [22, Table I]. Unless otherwise stated, the following parameters are used: $M = 80$, $N_{rx} = N_{tx} = 5$, $L_u = L_d = 20$, and $\frac{\rho_{SI}^2}{N_o} = 40$ dB. The powers are set as $\tilde{p}_\tau = \tilde{P}_{u,l}^{MAX} = 100$ mW and $\tilde{P}_{d,m}^{MAX} = 200$ mW.

A. Achievable Spectral Efficiency

The achievable SE as a function of the APs M, UL/DL transmit powers, quantization bits, and residual SI/IAI is investigated. Here, we assume the l-th UL user transmit at full power, i.e., $p_{u,l} = P_{u,l}^{MAX}, \forall l$ and the APs use equal power allocation, i.e., $\eta_{mk} = P_{d,m}^{MAX} / (N_{tx} \sum_{k=1}^{L_d} a_{mk}^d)$. The analytical SE of the l-th UL user and k-th DL user are obtained

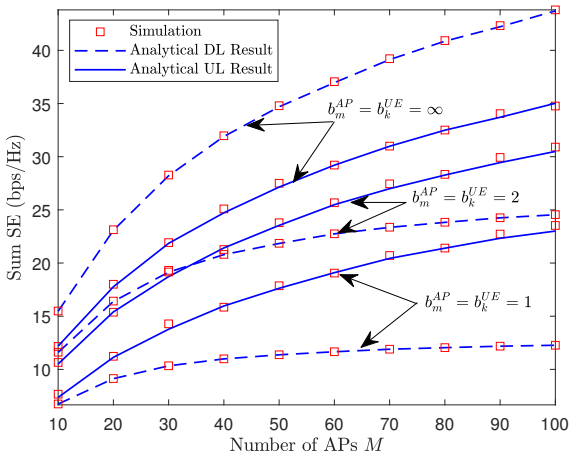

Fig. 3: Sum SE vs number of APs M ($L_u = L_d = 10$, $N_{rx} = N_{tx} = 2$).

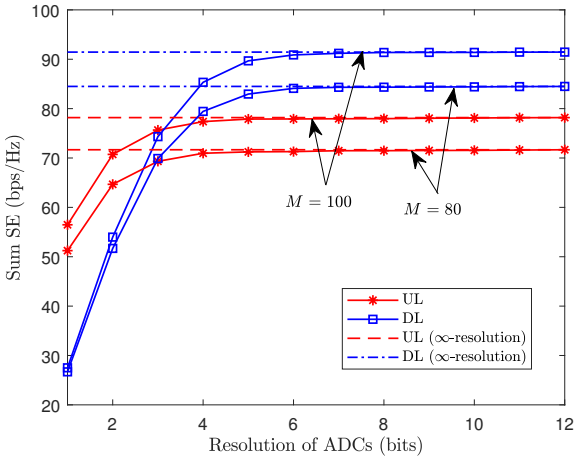

Fig. 4: Sum SE vs ADCs' resolution (bits) ($L_u = L_d = 30$, $N_{rx} = N_{tx} = 5$).

according to (6) and (7), respectively. The simulated UL and DL results are achieved by (4) and (5), respectively. The results are then aggregated over the L_u and L_d users to obtain the UL sum SE and DL sum SE, respectively. The total sum SE is then achieved by adding the UL sum SE and the DL sum SE.

Fig. 2 shows plots of the simulated total sum SE and analytical results versus the transmit power, for different M.[9] The UL/DL powers are jointly varied from -40 dBm to 30 dBm. From Fig. 2, it is noted that the analytical results match tightly with the Monte-Carlo simulations which confirms the validity of Theorems 1 and 2. The total sum SE of the FD CF mMIMO generally increases with the increase in the number of APs M and improves as the transmit powers increase until saturation. This saturation is caused by the growth in the MUI, residual SI/IAI, UL-to-DL, and influence of the QN whose effects are increasing functions of power (see (8) and (9)). We also observe that for any given transmit power and M, the total sum SE is higher in the Rician fading environments than the Rayleigh case.

In Fig. 3, we plot the simulated achievable UL/DL sum SE, analytical UL results, and analytical DL results against the number of APs M, for different ADC resolutions b_m^{AP} and b_k^{UE}, where $L_u = L_d = 10$ and $N_{rx} = N_{tx} = 2$. It is obvious from Fig. 3 that the analytical results are again exact. The UL and DL sum SEs increase with the growth in M and reduces as the ADCs' resolution declines. In the low-bit regime, the DL sum SE saturates rapidly as the APs increase since both the desired signal and QN of the k-th DL user grow at the same speed with M (see Theorem 2). However, the UL shows monotonic growth with M for any ADC resolution since the desired signal has a higher order than the QN (i.e., with respect to the receive arrays) as shown in Theorem 1. Since the analytical results are tight, from here on, the figures are generated with the closed-form solutions instead of the time-consuming Monte Carlo simulations.

Fig. 4 shows a plot of the UL/DL sum SE versus the quantization bits $b_m^{AP}(b_k^{UE})$, for different APs M. We set $L_u = L_d = 30$ and $\rho_{SI}^2/N_o = 80$ dB. It is observed that the UL and DL sum SEs grow as the ADCs' resolution increases until saturating to the perfect quantization case. For the UL, the FD CF mMIMO needs about 5 bit ADCs to converge to the infinite-resolution case while in the DL about 7 bits are required to achieve equal sum SE as the perfect quantization. We note that the UL shows better sum SE than the DL, in the low quantization bit regime. However, as the ADCs' resolution increases beyond 3 bits, the DL shows superior sum SE since the APs use higher transmit power (than the UL users) and DL users suffer less UL-to-DL interference compared with the residual SI/IAI at the APs. Note that for the DL, the QN dominates in the low-bit region. This result is consistent with Fig. 3.

Next, we study the impact of the residual SI/IAI and UL-to-DL interference on the achievable sum SE by plotting the total sum SE versus the normalized residual SI $\frac{\rho_{SI}^2}{N_o}$ in Fig. 5. For comparison, we include the total sum SEs of the co-located FD mMIMO and the HD modes. The HD result is obtained by setting the residual SI, IAI, and UL-to-DL interference to zero while doubling the transmit powers and imposing a 0.5 pre-log factor in the SE expressions (7) and (6), for fairness. It is observed that the total sum SE of the FD CF (and co-located) mMIMO reduces rapidly as the strength of the residual SI increases. For the HD, the sum SE remains unchanged as it is unaffected by the residual SI, IAI, and UL-to-DL interference. We note that the vulnerability of the FD CF mMIMO to the residual SI is aggravated by the low-resolution ADCs. For instance, with 1-bit quantization, the FD CF mMIMO outperforms the HD CF mMIMO in the region $\rho_{SI}^2/N_o \leq 143$ dB and the region grows to $\rho_{SI}^2/N_o \leq 152$ dB and $\rho_{SI}^2/N_o \leq 155$ dB for $b_m^{AP}(b_k^{UE}) = 3$ and $b_m^{AP}(b_k^{UE}) = \infty$, respectively. For the co-located mMIMO, the FD outperforms the HD in the regime $\rho_{SI}^2/N_o \leq 118$ dB, $\rho_{SI}^2/N_o \leq 126$ dB and $\rho_{SI}^2/N_o \leq 134$

[9]For comparison, we include the achievable SE in Rayleigh fading scenarios which are obtained by setting the Rician κ-factors in the AP-user links to zero, i.e., $\kappa_{mk} = \kappa_{ml} = 0, \forall m, k, l$.

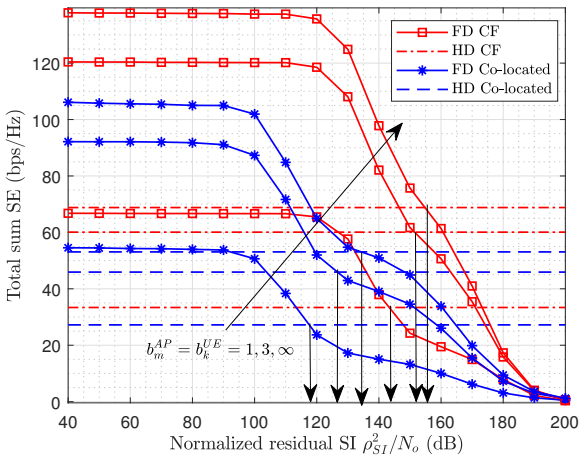

Fig. 5: Total sum SE vs residual SI $\frac{\rho_{SI}^2}{N_o}$ (dB) ($M = 80$, $N_{rx} = N_{tx} = 5$, $L_u = L_d = 20$).

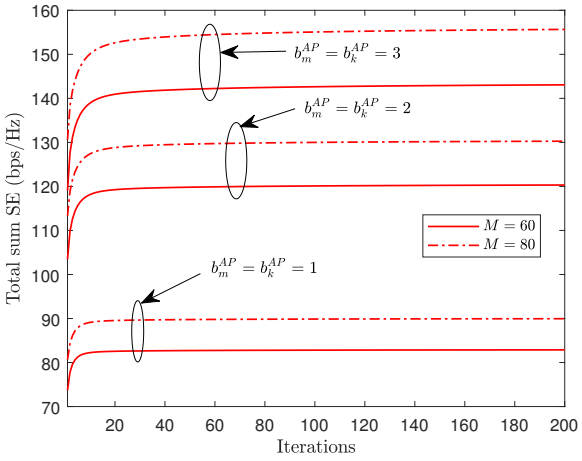

Fig. 7: Convergence of the proposed sum SE maximization algorithm ($L_u = L_d = 30$).

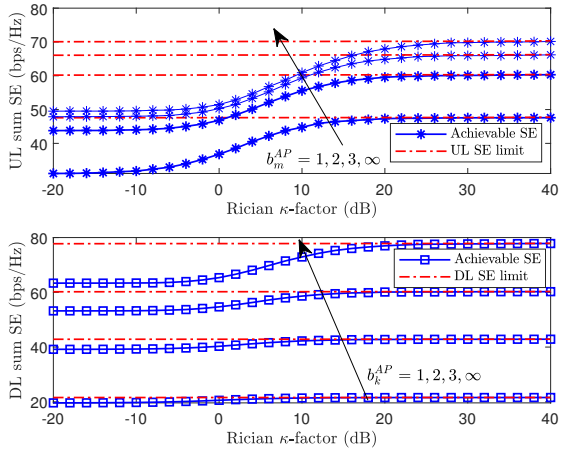

Fig. 6: Sum SE vs Rician κ-factor (dB) ($M = 80$, $L_u = L_d = 30$).

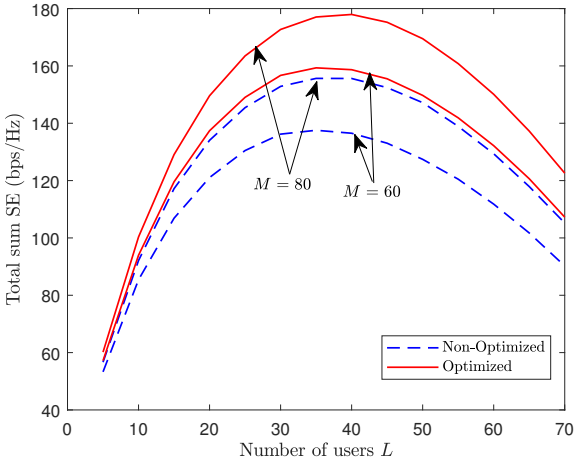

Fig. 8: Total sum SE vs number of users ($\frac{\rho_{SI}^2}{N_o} = 80$ dB, $b_m^{AP} = 3$, and $b_k^{UE} = 5$).

dB for ADC resolutions 1, 3 and ∞, respectively. Thus, the FD CF mMIMO provides more resistance to the residual SI than its co-located counterpart. Moreover, the total sum SE is substantially higher for the FD CF mMIMO than the co-located counterpart. This is because the IAI is considerably lower (due to the higher pathloss among the APs) than the SI at the co-located mMIMO, where the receive and transmit antenna arrays are in close proximity.

Fig. 6 shows a plot of the UL/DL sum SE versus the Rician κ-factor in dB. We set $L_u = L_d = 30$. Here, the UL and DL Rician κ-factors are set such that $\kappa_{ml} = \kappa_{mk} = \kappa, \forall m, l, k$. The upper subplot shows the UL sum SE while the lower subplot indicates the DL sum SE. We observe that the UL/DL sum SEs show an initial growth as the κ increases until it approaches a saturation point. This point of convergence is obtained by (10) and (11) for the UL and DL, respectively. Thus, in a strong LoS environment, there exists a performance ceiling irrespective of the channel estimation quality. Further, it is noted that the rate of saturation is influenced strongly by the ADCs' resolution. For example, in the UL, it is observed that for $b_m^{AP} = 1$ bit, the sum SE saturates at $\kappa = 18$ dB while the saturation point is $\kappa = 26$ dB for $b_m^{AP} = 3$ bits.

B. Power Optimization

Here, we discuss the convergence properties of the proposed algorithm and sum SE improvement thanks to the joint power allocation algorithm. We set the following parameters: $L_u = L_d = 30$, $\frac{\rho_{SI}^2}{N_o} = 80$ dB, $b_m^{AP} = 3$, $\forall m$ and $b_k^{UE} = 5$, $\forall k$.

Fig. 7 indicates the convergence of the proposed sum SE maximization algorithm, for different APs M and ADCs' resolution b_m^{AP} (b_k^{UE}). Algorithm 2 for alternating optimization for (17) comprises the WMMSE outer loop and an inner loop for the ADMM. From the figure, it is observed that for every update of the data powers, the total sum SE of the network is improved. From an initial starting point, the system sees about 12% to 20% growth in the total sum SE at the point of convergence (for all the considered APs and quantization bits).

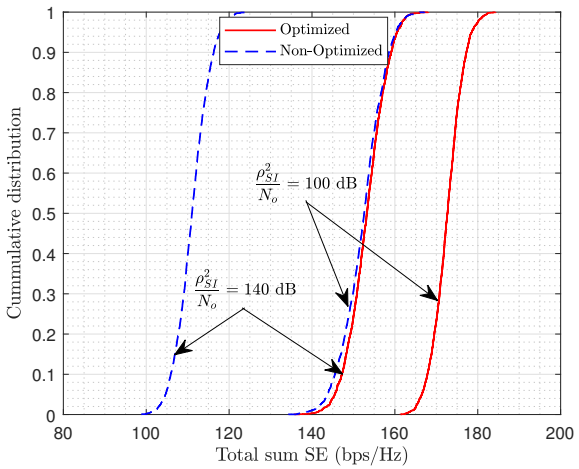

Fig. 9: CDF of total sum SE ($M = 80$, $N_{rx} = N_{tx} = 5$, $L_u = L_d = 30$, $b_m^{AP} = 3$, $b_k^{UE} = 5$).

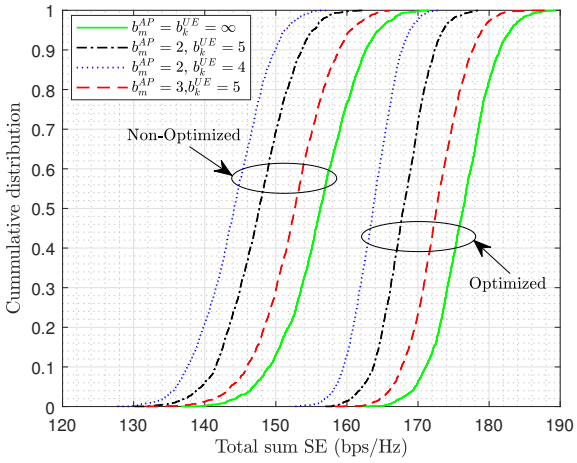

Fig. 10: CDF of total sum SE ($M = 80$, $N_{rx} = N_{tx} = 5$, $L_u = L_d = 30$, and $\frac{\rho_{SI}^2}{N_o} = 80$ dB).

We note that the proposed algorithm requires few iterations to converge. Meanwhile, the algorithm has low complexity since each step in the algorithms involves solving closed-form expression.

In Fig. 8, we compare the performance of the FD CF mMIMO with low-resolution ADCs and power optimization (i.e., indicated as "Optimized") with the setting without power optimization (i.e., shown as "Non-Optimized"). We plot the total sum SE versus the number of UL/DL users, for different M. It is considered that $L_u = L_d = L$, i.e., the total number of UL and DL users in the network is $2L$. From Fig. 8, we observe that jointly optimizing the data powers offers significant improvements in the total sum SE. For e.g., when $M = 80$, the SE improvement with $L = 5$ is 6.18% which increases to 13.7% for $L = 35$. It is worth noting that the "Optimized" system with $M = 60$ shows better sum SE than the setting with $M = 80$ without optimization. This shows the robust SE improvement provided by the joint power optimization algorithm. Generally, the total sum SE decays as the users increase beyond a certain number due to the pre-log factor τ_s/τ_c. As the number of users increase, more timeslots are utilized for pilot signaling which results in reduction of the available slots for useful data transmission.

Fig. 9 shows the cumulative distribution function (CDF) of the total sum SE for the "Optimized" and "Non-Optimized" system, for different levels of normalized residual SI ρ_{SI}^2/N_o. The performance gains introduced by the power allocation algorithm at $\rho_{SI}^2/N_o = 100$ dB and $\rho_{SI}^2/N_o = 140$ dB are 13.2% and 38%, respectively. We note that the sum SE reduction due to the increase in ρ_{SI}^2/N_o (i.e., from 100 dB to 140 dB) is 12.7% in the "Optimized" system and 37.5% in the "Non-Optimized" setting. Thus, indicating that the power optimization provides more robustness to the increasing interference caused by the FD transmissions. In Fig. 10, we plot the CDF of the total sum SE with and without power optimization, for the quantized and unquantized FD CF mMIMO. It is clear that the power allocation algorithm provides significant boost in the total sum SE. Notably, the quantized FD CF system with power allocation shows better total sum SE than the unquantized FD CF mMIMO without optimization.

C. Energy Efficiency

In this subsection, we evaluate the performance of the FD CF mMIMO with low-resolution ADCs by investigating the trade-off between the power consumption and the achievable SE. First, we modify a generic power consumption model proposed in [40], [41], [42] for the FD CF mMIMO. Then, this power consumption model is used to evaluate the UL and DL EEs. The total circuit power consumed by the RF chains in the UL and DL are modeled by

$$P_T^u = MN_{rx}(P_{LNA} + P_M + P_{LPF} + P_{LO} + P_{Bamp}) + 2N_{rx}\sum_{m=1}^{M}(cP_{AGC,m} + P_{ADC,m}), \quad (37)$$

$$P_T^d = L_d(P_{LNA} + P_M + P_{LPF} + P_{LO} + P_{Bamp}) + \sum_{k=1}^{L_d}(cP_{AGC,k} + P_{ADC,k}), \quad (38)$$

respectively, where P_{LNA}, P_M, P_{LO}, P_{LPF}, P_{Bamp}, $P_{AGC,m}$, and$P_{ADC,m}$ denote the power consumed by the low-noise amplifier, mixer, local oscillator, low-pass filter, baseband amplifier, m-th AP automatic gain controller (AGC), and ADC, respectively; $P_{AGC,k}$ and $P_{ADC,k}$ are the power consumption of the AGC and ADC at the k-th DL user, respectively. Also, c is an indicator which takes the value $c = 0$, for $b_m^{AP} = 1$; $c = 1$, for $b_m^{AP} > 1$. The power consumed by the ADCs is given by $P_{ADC,m} = 2^{b_m^{AP}} F_W f_s$, where F_W denotes the Walden's figure-of-merit (FOM) and f_s is the Nyquist sampling rate. Similar definition holds for $P_{ADC,k}$. Using (37) and (38), the UL/DL EE is given by $\vartheta_{EE}^v = B\sum_{k=1}^{L_v} R_k^v/P_T^v$ bits/Joule [30], where B denotes

the bandwidth and $v \in [u, d]$.[10] For numerical evaluation, the following power consumption values are used: $P_M = 16.8$ mW, $P_{LO} = 5$ mW, $P_{LPF} = 14$ mW, $P_{Bamp} = 5$ mW, $P_{LNA} = 39$ mW [42] and $P_{AGC} = 2$ mW [40], [41] with $F_W = 494$ fJ/step/Hz [42].[11]

Fig. 11 (a) shows a plot of UL EE (in Mbps/J) versus the ADCs' resolution b_m^{AP}, for different number of APs M. For comparison, the EE performance in Rayleigh fading scenario is included. We set $L_u = L_d = 30$ and $\frac{\rho_{SI}^2}{N_o} = 80$ dB. It is observed that the UL EE monotonically increases as the ADCs' resolution increases from $b^{AP} = 1$ to 3. However, as b^{AP} increases beyond 3 bits, the UL EE declines rapidly towards zero. This is because the UL sum SE grows sublinearly with the ADCs' resolution while the power consumption increases exponentially with b^{AP}. Thus, as b^{AP} increases above a threshold, i.e., $b^{AP} > 3$, the power consumed dominates and the EE decays rapidly. Generally, the UL EE reduces as M grows since the increase in the receive RF chains implies more ADCs are employed. We note that the total power consumed grows linearly with M and N_{rx} while the UL sum SE grows logarithmically with the APs. Furthermore, it is obvious from Fig. 11 (a) that the UL EE in Rician fading channels is superior to the Rayleigh case. This is because the UL sum SE improves in strong LoS environments whereas the total power consumed by the ADCs is independent of the Rician κ-factor (see Fig. 6). Fig. 11 (b) plots the trade-off between the UL EE and sum SE. We vary the quantization bits from $b^{AP} = 1$ to 12. For each b^{AP}, the UL sum SE and EE are computed. Higher sum SE are plotted on the right while higher EE performance are shown in the upper plots. Therefore, the best EE/SE trade-off occur on the right uppermost points. It is observed that as the ADCs' resolution increases, both the UL EE and sum SE increases as b^{AP} improves from 1 to 3. For $b^{AP} > 3$, the UL EE reduces while the UL sum SE remains saturated. Also, the entire operating region envelope of the FD CF mMIMO with low-resolution ADCs is improved in Rician fading scenarios.

Fig. 11(c) plots the DL EE against the ADCs' resolution b^{UE} at the DL users, for different M. It is observed that the DL EE initially grows as b^{UE} increases from 1 to 4 before decaying towards zero. As the quantization bits at the DL users improves, the DL sum SE grows until saturation. However, the power consumption increases exponentially for every increase in the resolution bits and the EE subsequently falls. Contrasting with the UL, the DL EE improves as the number of APs increases since the DL sum SE enhances with M and the total power consumption in the DL, i.e., P_T^d is not dependent on the number of transmit RF chains, i.e., M and N_{tx}. Similar to the UL, the DL EE is improved in Rician channels when compared with the Rayleigh case. Fig. 11(d) provides insights into the DL EE and SE trade-off. From Fig. 11, it is clear that the DL EE and sum SE increases as the quantization bits increase from $b^{UE} = 1$ to 4. However, for $b^{UE} > 4$, the DL sum SE remains flat while the DL EE decreases towards zero as the power consumed by the DL users dominates. Also, the envelope of the operating region in the DL increases as M grows and enlarges in LoS conditions. From Fig. 11(a) and Fig. 11(c), we note that using the derived analytical results, we can numerically obtain the optimal number of quantization bits that maximize the UL and DL EEs, i.e., $b^{AP} = 3$ and $b^{UE} = 4$, respectively.

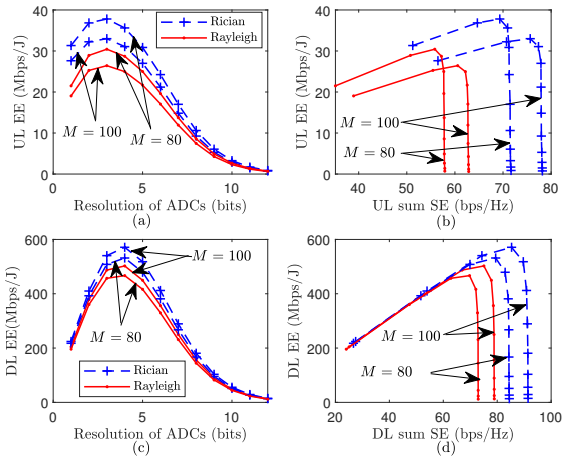

Fig. 11: (a) UL: EE vs ADCs' resolution. (b) UL: EE/SE trade-off. (c) DL: EE vs ADCs' resolution. (d) DL: EE/SE trade-off.

VI. Conclusion

We have studied the SE/EE of the FD CF mMIMO with low-resolution ADCs over Rician channels. Closed-form solutions have been derived to characterize the joint effects of the Rician κ-factor, UL/DL powers, residual SI/IAI, UL-to-DL interference, and QN on the UL/DL achievable SEs. The vulnerability of the FD system to the residual SI/IAI and UL-to-DL interference is aggravated by the coarse quantization. However, the FD CF mMIMO offers significant SE improvement over the HD counterpart and co-located FD mMIMO. We have maximized the total sum SE of the network subject to the per user power and per AP power constraints. From the results, the proposed algorithm offers considerable SE gain over the uniform power allocation. We have analyzed the trade-off between the SE and EE as a function of the ADCs' resolution. The optimal ADC resolution that maximizes the EE can be numerically achieved.

Appendix A
Proof of Theorem 1

1) Solve for Desired Signal and Noise: Here, we have the desired signal $A_l^u \triangleq p_{u,l}|\mathbb{E}\{\sum_{m=1}^{M} \alpha_m \hat{\mathbf{h}}_{ml}^H \mathbf{h}_{ml}\}|^2$, where $\mathbb{E}\{\sum_{m=1}^{M} \alpha_m \hat{\mathbf{h}}_{ml}^H \mathbf{h}_{ml}\}$ is rewritten as $\sum_{m=1}^{M} \alpha_m \mathbb{E}\{\hat{\mathbf{h}}_{ml}^H \mathbf{h}_{ml}\}$.

$$\mathbb{E}\{\hat{\mathbf{h}}_{ml}^H \mathbf{h}_{ml}\} = \mathbb{E}\{\hat{\mathbf{h}}_{ml}^H (\tilde{\mathbf{h}}_{ml} + \hat{\mathbf{h}}_{ml})\} \overset{(a)}{=} \mathbb{E}\{\|\hat{\mathbf{h}}_{ml}\|^2\}$$
$$= \mathbb{E}\{\|\kappa_{ml}^{1/2} \bar{\kappa}_{ml}^{-1/2} \mathbf{h}_{L,ml} + \bar{\kappa}_{ml}^{-1/2} \hat{\mathbf{h}}_{w,mk}\|^2\}$$
$$\overset{(b)}{=} \kappa_{ml} \bar{\kappa}_{ml}^{-1} \mathbb{E}\{\|\mathbf{h}_{L,mk}\|^2\} + \bar{\kappa}_{ml}^{-1} \mathbb{E}\{\|\hat{\mathbf{h}}_{w,ml}\|^2\}, \quad (39)$$

[10] Since the key benefit of using low-resolution ADCs in mMIMO systems is to reduce the circuit power consumption, particularly due to the ADCs, we study the EE as a function of the circuit power consumption and ignore the UL/DL transmit powers. This is a standard assumption in the literature [16], [30], [41], [42].

[11] This corresponds to the high power ADC which operates at a speed of 1 Gs/s. The Walden's FOM can have values as small as $F_W = 5 \sim 65$ fJ/step/Hz for a low-to-intermediate power ADC [42].

where (a) uses the fact that the estimate and error channel vectors are independent and in (b), we remove all the terms with zero expectations. Then, we have $\mathbb{E}\{\|\mathbf{h}_{L,mk}\|^2\} = \zeta_{ml}\sum_{n=1}^{N_{rx}} e^{j(n-1)\pi\sin(\psi^u_{ml})} \cdot e^{-j(n-1)\pi\sin(\psi^u_{ml})} = \zeta_{ml}N_{rx}$ and $\mathbb{E}\{\|\hat{\mathbf{h}}_{w,ml}\|^2\} = \zeta_{ml}\mu_{ml}N_{rx}$. Therefore, we have the solution $p_{u,l}N_{rx}^2(\sum_{m=1}^{M}\alpha_m\zeta_{ml}\bar{\kappa}_{ml}^{-1}(\kappa_{ml}+\mu_{ml}))^2$. Similarly, the noise term yields $\sum_{m=1}^{M}\alpha_m^2\mathbb{E}\{\|\hat{\mathbf{h}}_{ml}\|^2\} = \sum_{m=1}^{M}\alpha_m^2\zeta_{ml}\bar{\kappa}_{ml}^{-1}(\kappa_{ml}+\mu_{ml})$.

2) Solve the BUG: The term B_l^u is rewritten as $p_{u,l}[\sum_{m=1}^{M}\sum_{m'=1}^{M}\alpha_m\alpha_{m'}\mathbb{E}\{\hat{\mathbf{h}}_{ml}^H\mathbf{h}_{ml}\mathbf{h}_{m'l}^H\hat{\mathbf{h}}_{m'l}\} - N_{rx}^2(\sum_{m=1}^{M}\alpha_m\zeta_{ml}\bar{\kappa}_{ml}^{-1}(\kappa_{ml}+\mu_{ml}))^2]$. Here, we derive the first term for all possible AP combinations.

For $m \neq m'$, $\mathbb{E}\{\hat{\mathbf{h}}_{ml}^H\mathbf{h}_{ml}\mathbf{h}_{m'l}^H\hat{\mathbf{h}}_{m'l}\} = \mathbb{E}\{\hat{\mathbf{h}}_{ml}^H\mathbf{h}_{ml}\}\mathbb{E}\{\mathbf{h}_{m'l}^H\hat{\mathbf{h}}_{m'l}\}$. $\mathbb{E}\{\hat{\mathbf{h}}_{ml}^H\mathbf{h}_{ml}\} = \mathbb{E}\{\hat{\mathbf{h}}_{ml}^H\hat{\mathbf{h}}_{ml}\} = \zeta_{ml}\bar{\kappa}_{ml}^{-1}(\kappa_{ml}+\mu_{ml})N_{rx}$. Similarly, $\mathbb{E}\{\mathbf{h}_{m'l}^H\mathbf{h}_{m'l}\} = \zeta_{m'l}\bar{\kappa}_{m'l}^{-1}(\kappa_{m'l}+\mu_{m'l})N_{rx}$.

For $m = m'$, we have $\mathbb{E}\{|\hat{\mathbf{h}}_{ml}^H\mathbf{h}_{ml}|^2\} = \mathbb{E}\{|\hat{\mathbf{h}}_{ml}^H\tilde{\mathbf{h}}_{ml}|^2\} + \mathbb{E}\{|\hat{\mathbf{h}}_{ml}^H\hat{\mathbf{h}}_{ml}|^2\}$. Thus, $\mathbb{E}\{|\hat{\mathbf{h}}_{ml}^H\mathbf{h}_{ml}|^2\} = \tilde{\zeta}_{ml}\mathbb{E}\{\|\mathbf{h}_{ml}\|^2\} = \tilde{\zeta}_{ml}\zeta_{ml}\bar{\kappa}_{ml}^{-1}(\kappa_{ml}+\mu_{ml})N_{rx}$. For $\mathbb{E}\{|\hat{\mathbf{h}}_{ml}^H\hat{\mathbf{h}}_{ml}|^2\}$, we can write

$$\mathbb{E}\{\|\hat{\mathbf{h}}_{ml}\|^4\} = \mathbb{E}\{\|(\kappa_{ml}^{1/2}\bar{\kappa}_{ml}^{-1/2}\mathbf{h}_{L,ml}^H + \bar{\kappa}_{ml}^{-1/2}\hat{\mathbf{h}}_{w,mk}^H)\times (\kappa_{ml}^{1/2}\bar{\kappa}_{ml}^{-1/2}\mathbf{h}_{L,ml} + \bar{\kappa}_{ml}^{-1/2}\hat{\mathbf{h}}_{w,mk})\|^2\} \overset{(c)}{=} \kappa_{ml}^2\bar{\kappa}_{ml}^{-2}\mathbb{E}\{|\mathbf{h}_{L,ml}|^4\} + \kappa_{ml}\bar{\kappa}_{ml}^{-2}\mathbb{E}\{|\mathbf{h}_{L,ml}^H\hat{\mathbf{h}}_{w,ml}|^2\} + \kappa_{ml}\bar{\kappa}_{ml}^{-2}\mathbb{E}\{|\hat{\mathbf{h}}_{w,ml}^H\mathbf{h}_{L,ml}|^2\} + \kappa_{ml}\bar{\kappa}_{ml}^{-2}\mathbb{E}\{|\mathbf{h}_{L,ml}^H\mathbf{h}_{L,ml}\hat{\mathbf{h}}_{w,ml}^H\hat{\mathbf{h}}_{w,ml}|\} + \kappa_{ml}\bar{\kappa}_{ml}^{-2}\mathbb{E}\{|\hat{\mathbf{h}}_{w,ml}^H\hat{\mathbf{h}}_{w,ml}\mathbf{h}_{L,ml}^H\mathbf{h}_{L,ml}|\} + \bar{\kappa}_{ml}^{-2}\mathbb{E}\{\|\hat{\mathbf{h}}_{w,ml}\|^4\},$$

where in (c), we remove all the terms with zero expectations.

From above, we derive $\mathbb{E}\{\|\mathbf{h}_{L,ml}\|^4\} = (\zeta_{ml}\sum_{n=1}^{N_{rx}} e^{j(n-1)\pi\sin(\psi^u_{ml})}\cdot e^{-j(n-1)\pi\sin(\psi^u_{ml})})^2 = \zeta_{ml}^2N_{rx}^2$, $\mathbb{E}\{|\mathbf{h}_{L,ml}^H\hat{\mathbf{h}}_{w,ml}|^2\} = \zeta_{ml}^2\mu_{ml}N_{rx}$, and $\mathbb{E}\{|\hat{\mathbf{h}}_{w,ml}^H\mathbf{h}_{L,ml}|^2\} = \zeta_{ml}^2\mu_{ml}N_{rx}$. Also, $\mathbb{E}\{|\mathbf{h}_{L,ml}^H\mathbf{h}_{L,ml}\hat{\mathbf{h}}_{w,ml}^H\hat{\mathbf{h}}_{w,ml}|\} = \mathbb{E}\{\mathbf{h}_{L,ml}^H\mathbf{h}_{L,ml}\}\mathbb{E}\{\hat{\mathbf{h}}_{w,ml}^H\hat{\mathbf{h}}_{w,ml}\} = \zeta_{ml}^2\mu_{ml}N_{rx}^2$. Similarly, $\mathbb{E}\{|\hat{\mathbf{h}}_{w,ml}^H\hat{\mathbf{h}}_{w,ml}\mathbf{h}_{L,ml}^H\mathbf{h}_{L,ml}|\} = \zeta_{ml}^2\mu_{ml}N_{rx}^2$. Using [43, Lemma 2.9], $\mathbb{E}\{\|\hat{\mathbf{h}}_{w,ml}\|^4\} = \zeta_{ml}^2\mu_{ml}^2N_{rx}(N_{rx}+1)$. Thus,

$$\mathbb{E}\Big\{\Big|\sum_{m=1}^{M}\alpha_m\hat{\mathbf{h}}_{ml}^H\mathbf{h}_{ml}\Big|^2\Big\} = \sum_{m=1}^{M}\alpha_m^2\Big[\tilde{\zeta}_{ml}\zeta_{ml}\bar{\kappa}_{ml}^{-1}(\kappa_{ml}+\mu_{ml})\times N_{rx} + \bar{\kappa}_{ml}^{-2}\zeta_{ml}^2(\kappa_{ml}^2N_{rx}^2 + 2\kappa_{ml}\mu_{ml}N_{rx} + 2\kappa_{ml}\mu_{ml}N_{rx}^2 + \mu_{ml}^2N_{rx}^2 + \mu_{ml}^2N_{rx})\Big] + \sum_{m\neq m'}^{M}\sum_{m'=1}^{M}\alpha_m\alpha_{m'}\zeta_{ml}\bar{\kappa}_{ml}^{-1}\zeta_{m'l}\bar{\kappa}_{m'l}^{-1}\times \Big(\kappa_{ml}\kappa_{m'l} + \mu_{ml}\mu_{m'l} + \kappa_{ml}\mu_{m'l} + \mu_{ml}\kappa_{m'l}\Big)N_{rx}^2$$

$$= N_{rx}\sum_{m=1}^{M}\alpha_m^2\bar{\kappa}_{ml}^{-1}\zeta_{ml}\Big[\tilde{\zeta}_{ml}(\kappa_{ml}+\mu_{ml}) + \bar{\kappa}_{ml}^{-1}\zeta_{ml}(2\kappa_{ml}\mu_{ml} + \mu_{ml}^2)\Big] + N_{rx}^2\sum_{m=1}^{M}\sum_{m'=1}^{M}\alpha_m\alpha_{m'}\zeta_{ml}\bar{\kappa}_{ml}^{-1}\zeta_{m'l}\bar{\kappa}_{m'l}^{-1}\Big(\kappa_{ml}\kappa_{m'l} + \mu_{ml}\mu_{m'l} + \kappa_{ml}\mu_{m'l} + \mu_{ml}\kappa_{m'l}\Big).$$

Using $\tilde{\zeta}_{ml} = \zeta_{ml}\bar{\kappa}_{ml}^{-1} - \hat{\zeta}_{ml}$ and performing simple algebra $p_{u,l}\text{Var}(\sum_{m=1}^{M}\alpha_m\hat{\mathbf{h}}_{ml}^H\mathbf{h}_{ml})$ yields

$$p_{u,l}N_{rx}\sum_{m=1}^{M}\alpha_m^2\bar{\kappa}_{ml}^{-2}\zeta_{ml}^2(\mu_{ml}+\kappa_{ml}+\mu_{ml}\kappa_{ml}). \tag{40}$$

3) Solve for the MUI: The MUI term is expressed as $C_{ll'} = \sum_{l'\neq l}^{K_u}\sum_{m=1}^{M}p_{u,l'}\alpha_m^2\mathbb{E}\{|\hat{\mathbf{h}}_{ml}^H\mathbf{h}_{ml'}|^2\}$. We expand $\mathbb{E}\{|\hat{\mathbf{h}}_{ml}^H\mathbf{h}_{ml'}|^2\} = \mathbb{E}\{|(\bar{\kappa}_{ml}^{-1/2}\kappa_{ml}^{1/2}\mathbf{h}_{L,ml}^H + \bar{\kappa}_{ml}^{-1/2}\hat{\mathbf{h}}_{w,ml}^H)(\bar{\kappa}_{ml'}^{-1/2}\kappa_{ml'}^{1/2}\mathbf{h}_{L,ml'} + \bar{\kappa}_{ml'}^{-1/2}\mathbf{h}_{w,ml'})|^2\}$ $= \bar{\kappa}_{ml}^{-1}\bar{\kappa}_{ml'}^{-1}[\kappa_{ml}\kappa_{ml'}\mathbb{E}\{|\mathbf{h}_{L,ml}^H\mathbf{h}_{L,ml'}|^2\} + \kappa_{ml}\mathbb{E}\{|\mathbf{h}_{L,ml}^H\mathbf{h}_{w,ml'}|^2\} + \kappa_{ml'}\mathbb{E}\{|\hat{\mathbf{h}}_{w,ml}^H\mathbf{h}_{L,ml'}|^2\} + \mathbb{E}\{|\hat{\mathbf{h}}_{w,ml}^H\times \mathbf{h}_{w,ml'}|^2\}]$. The following expectations are derived: $\mathbb{E}\{|\hat{\mathbf{h}}_{w,ml}^H\mathbf{h}_{w,ml'}|^2\} = \zeta_{ml}\mu_{ml}\zeta_{ml'}N_{rx}$, $\mathbb{E}\{|\mathbf{h}_{L,ml}^H\mathbf{h}_{w,ml'}|^2\} = \zeta_{ml'}\zeta_{ml}N_{rx}$, and $\mathbb{E}\{|\hat{\mathbf{h}}_{w,ml}^H\mathbf{h}_{L,ml'}|^2\} = \zeta_{ml'}\zeta_{ml}\mu_{ml}N_{rx}$. Also, $\mathbb{E}\{|\mathbf{h}_{L,ml}^H\mathbf{h}_{L,ml'}|^2\} = [\sum_{n=1}^{N_{rx}}e^{j(n-1)\pi(\sin(\psi^u_{ml})-\sin(\psi^u_{ml'}))}]^2\zeta_{ml}\zeta_{ml'} \overset{(d)}{=} \zeta_{ml}\zeta_{ml'}[\phi_{mll'}e^{j(\frac{\pi}{2}(N_{rx}-1))(\sin(\psi^u_{ml})-\sin(\psi^u_{ml'}))}]^2 = \zeta_{ml}\zeta_{ml'}\phi_{mll'}^2$, where (d) uses [24, eq. (118)]. Combining all derived terms, the MUI term achieves

$$N_{rx}\sum_{l'\neq l}^{L_u}\sum_{m=1}^{M}p_{u,l'}\alpha_m^2\zeta_{ml}\zeta_{ml'}\bar{\kappa}_{ml}^{-1}\bar{\kappa}_{ml'}^{-1}(\kappa_{ml}\kappa_{ml'}\frac{\phi_{mll'}^2}{N_{rx}} + \kappa_{ml} + \kappa_{ml'}\mu_{ml} + \mu_{ml}). \tag{41}$$

4) Solve the residual SI and IAI: : The residual SI/IAI is given as $\sum_{k=1}^{L_d}\sum_{m=1}^{M}\sum_{n=1}^{M}\alpha_m^2\eta_{nk}\mathbb{E}\{|\hat{\mathbf{h}}_{ml}^H\mathbf{Q}_{mn}\hat{\mathbf{g}}_{nk}|^2\}$. We derive $\mathbb{E}\{|\hat{\mathbf{h}}_{ml}^H\mathbf{Q}_{mn}\hat{\mathbf{g}}_{nk}|^2\} = \beta_{nk}\kappa_{nk}\bar{\kappa}_{nk}^{-1}(\nu_{nk}+\kappa_{nk})\mathbb{E}\{|\hat{\mathbf{h}}_{ml}^H\mathbf{Q}_{mn}\mathbf{Q}_{mn}^H\hat{\mathbf{h}}_{ml}|\} = N_{tx}N_{rx}\beta_{nk}\kappa_{nk}\bar{\kappa}_{nk}^{-1}(\nu_{nk}+\kappa_{nk})\sigma_{mn}^2\zeta_{ml}\kappa_{ml}\bar{\kappa}_{ml}^{-1}(\mu_{ml}+\kappa_{ml})$. Thus, we have

$$\sum_{k=1}^{L_d}\sum_{m=1}^{M}\sum_{n=1}^{M}\alpha_m^2\eta_{nk}\sigma_{mn}^2\beta_{nk}\kappa_{nk}\bar{\kappa}_{nk}^{-1}\zeta_{ml}\kappa_{ml}\bar{\kappa}_{ml}^{-1}(\nu_{nk}+\kappa_{nk})\times(\mu_{ml}+\kappa_{ml})N_{tx}N_{rx}. \tag{42}$$

5) Solve the QN: To derive the QN, we write $\mathbb{E}\{|\sum_{m=1}^{M}\hat{\mathbf{h}}_{ml}^H\tilde{\mathbf{z}}_m|^2\} = \sum_{m=1}^{M}\sum_{m'=1}^{M}\mathbb{E}\{|\hat{\mathbf{h}}_{ml}^H\tilde{\mathbf{z}}_m\tilde{\mathbf{z}}_{m'}\hat{\mathbf{h}}_{m'l}|\}$. For $m \neq m'$, $\mathbb{E}\{|\hat{\mathbf{h}}_{ml}^H\tilde{\mathbf{z}}_m\tilde{\mathbf{z}}_{m'}\hat{\mathbf{h}}_{m'l}|\} = 0$ since the QN vectors are uncorrelated. If $m = m'$, we have $\mathbb{E}\{|\hat{\mathbf{h}}_{ml}^H\mathbf{R}_{\tilde{\mathbf{z}}_m}\hat{\mathbf{h}}_{ml}|\}$. To obtain $\mathbf{R}_{\tilde{\mathbf{z}}_m}$, we derive $\mathbb{E}\{\mathbf{y}_m^u(\mathbf{y}_m^u)^H\} = \mathbb{E}\Big\{\sum_{l=1}^{L_u}\sum_{l'=1}^{L_u}\sqrt{p_{u,l}p_{u,l'}}\mathbf{h}_{ml}\mathbf{h}_{ml'}^H + \sum_{k=1}^{L_d}\sum_{k'=1}^{L_d}\sum_{n=1}^{M}\sum_{n'=1}^{M}\sqrt{\eta_{nk}\eta_{n'k'}}\mathbf{Q}_{mn}\hat{\mathbf{g}}_{nk}\hat{\mathbf{g}}_{n'k'}^H\mathbf{Q}_{mn'}^H\Big\} + \mathbf{I}_{N_{rx}}$. For $l \neq l'$, $\mathbb{E}\{|\mathbf{h}_{ml}\mathbf{h}_{ml'}^H|\} = 0$. If $n \neq n'$ and $k \neq k'$, $\mathbb{E}\{\mathbf{Q}_{mn}\hat{\mathbf{g}}_{nk}\hat{\mathbf{g}}_{n'k'}^H\mathbf{Q}_{mn'}^H\} = 0$; If $n = n$, $k \neq k'$, $\mathbb{E}\{|\mathbf{Q}_{mn}\hat{\mathbf{g}}_{nk}\hat{\mathbf{g}}_{nk'}^H\mathbf{Q}_{mn'}^H|\} = 0$; $n \neq n'$ and $k = k'$, $\mathbb{E}\{|\mathbf{Q}_{mn}\hat{\mathbf{g}}_{nk}\hat{\mathbf{g}}_{n'k}^H\mathbf{Q}_{mn'}^H|\} = 0$; Let $g_{nkt} = [\mathbf{g}_{nk}]_t$, $u_{it} = [\mathbf{Q}_{mn}]_{it}$ and $h_{mli} = [\mathbf{h}_{ml}]_i$. Thus, the QN simplifies as

$$\sum_{m=1}^{M}\bar{\alpha}_m\sum_{i=1}^{N_{rx}}\Big(\mathbb{E}\{|\hat{h}_{mli}|^2\} + \sum_{l\neq l'}^{L_u}p_{u,l'}\mathbb{E}\{|\hat{h}_{mli}^*h_{ml'i}|^2\} + p_{u,l}\mathbb{E}\{|\hat{h}_{mli}^*h_{mli}|^2\} + \sum_{k=1}^{Ld}\sum_{n=1}^{M}\sum_{t=1}^{N_{tx}}\eta_{nk}\mathbb{E}\{|\hat{h}_{mli}^*u_{it}\hat{g}_{nkt}|^2\}\Big).$$

We derive $\mathbb{E}\{|\hat{h}_{mil}|^2\} = \zeta_{ml}\bar{\kappa}_{ml}^{-1}(\mu_{ml}+\kappa_{ml})$ and $\mathbb{E}\{|\hat{h}_{mli}^*u_{it}\hat{g}_{nkt}|^2\} = \sigma_{mn}^2\beta_{nk}\bar{\kappa}_{nk}^{-1}(\nu_{nk}+\kappa_{nk})\bar{\kappa}_{ml}^{-1}\zeta_{ml}(\mu_{ml}+\kappa_{ml})$.

Next, we write $\mathbb{E}\{|\hat{h}_{mli}^*h_{mli}|^2\} = \mathbb{E}\{|\hat{h}_{mli}^*\tilde{h}_{mli}|^2\} + \mathbb{E}\{|\hat{h}_{mli}|^4\}$; $\mathbb{E}\{|\hat{h}_{mli}^*\tilde{h}_{mli}|^2\} = \tilde{\zeta}_{ml}\zeta_{ml}\bar{\kappa}_{ml}^{-1}(\kappa_{ml}+\mu_{ml})$ and $\mathbb{E}\{|\hat{h}_{mli}|^4\} \overset{(d)}{=} \bar{\kappa}_{ml}^{-2}(\kappa_{ml}^2\mathbb{E}\{|h_{L,mli}|^4\} + \mathbb{E}\{|\hat{h}_{w,mli}|^4\} + 4\kappa_{ml}\mathbb{E}\{|h_{L,mli}^*\hat{h}_{w,mli}|^2\}) = \kappa_{ml}^2\bar{\kappa}_{ml}^{-2}\zeta_{ml}^2 + 2\bar{\kappa}_{ml}^{-2}\zeta_{ml}^2\mu_{ml}^2 +$

$4\zeta_{ml}^2\mu_{ml}\kappa_{ml}\bar{\kappa}_{ml}^{-2}$, where (d) removes the terms with zero expectations. Thus, $\mathbb{E}\{|\hat{h}_{mli}^* h_{mli}|^2\} = \tilde{\zeta}_{ml}\zeta_{ml}\bar{\kappa}_{ml}^{-1}(\kappa_{ml} + \mu_{ml}) + \bar{\kappa}_{ml}^{-2}\zeta_{ml}^2(\kappa_{ml}^2 + 2\mu_{ml}^2 + 4\mu_{ml}\kappa_{ml}) = \bar{\kappa}_{ml}^{-2}\zeta_{ml}^2(\kappa_{ml}^2 + \mu_{ml}^2 + 3\mu_{ml}\kappa_{ml} + \kappa_{ml} + \mu_{ml})$.

Finally, $\mathbb{E}\{|\hat{h}_{mli}^* h_{ml'i}|^2\} = (\kappa_{ml}\kappa_{ml'}\mathbb{E}\{|h_{L,mli}^* h_{L,ml'i}|^2\} + \kappa_{ml}\mathbb{E}\{|h_{L,mli}^* h_{w,ml'i}|^2\} + \kappa_{ml'}\mathbb{E}\{|\hat{h}_{w,mli}^* h_{L,ml'i}|^2\} + \mathbb{E}\{|\hat{h}_{w,mli}^* h_{w,ml'i})|^2\})\bar{\kappa}_{ml}^{-1}\bar{\kappa}_{ml'}^{-1}$, where we derive $\mathbb{E}\{|h_{L,mli}^* h_{L,ml'i}|^2\} = \zeta_{ml}\zeta_{ml'}$, $\mathbb{E}\{|h_{L,mli}^* h_{w,ml'i}|^2\} = \zeta_{ml'}\zeta_{ml}$, $\mathbb{E}\{|\hat{h}_{w,mli}^* h_{L,ml'i}|^2\} = \zeta_{ml'}\zeta_{ml}\mu_{ml}$, and $\mathbb{E}\{|\hat{h}_{w,mli}^* h_{w,ml'i})|^2\} = \zeta_{ml'}\zeta_{ml}\mu_{ml}$. Therefore, $\mathbb{E}\{|\hat{h}_{mli}^* h_{ml'i}|^2\} = \zeta_{ml}\zeta_{ml'}\bar{\kappa}_{ml}^{-1}\bar{\kappa}_{ml'}^{-1}(\mu_{ml} + \kappa_{ml} + \kappa_{ml'}\mu_{ml} + \kappa_{ml}\kappa_{ml'})$.

Combining the terms, the QN yields

$$\sum_{m=1}^{M} N_{rx}\bar{\alpha}_m[\zeta_{ml}\bar{\kappa}_{ml}^{-1}(\mu_{ml} + \kappa_{ml}) + p_{u,l}\bar{\kappa}_{ml}^{-2}\zeta_{ml}^2(\kappa_{ml}^2 + \mu_{ml}^2 + 3\mu_{ml}\kappa_{ml} + \kappa_{ml} + \mu_{ml}) + \sum_{l'\neq l}^{L_u} p_{u,l'}\zeta_{ml}\zeta_{ml'}\bar{\kappa}_{ml}^{-1}\bar{\kappa}_{ml'}^{-1}(\mu_{ml} + \kappa_{ml} + \kappa_{ml'}\mu_{ml} + \kappa_{ml}\kappa_{ml'}) + N_{tx}\sum_{k=1}^{Ld}\sum_{n=1}^{M}\eta_{nk}\sigma_{mn}^2\beta_{nk}\bar{\kappa}_{nk}^{-1}\times \bar{\kappa}_{ml}^{-1}\zeta_{ml}(\nu_{nk} + \kappa_{nk})(\mu_{ml} + \kappa_{ml})]. \quad (43)$$

Substituting the derived terms into (4) completes the proof.

Appendix B
Proof of theorem 2

For brevity, we derive only the QN term at the k-th DL user. The other terms are obtained by following Appendix A. Here, the QN is $\tilde{Z}_k^d = (\varepsilon_k - \varepsilon_k^2)\mathbb{E}\{|y_k^d|^2\}$, where

$$\mathbb{E}\{|y_k^d|^2\} = 1 + \sum_{l=1}^{K_u}\sum_{l'=1}^{L_u}\sqrt{p_{u,l}p_{u,l'}}\mathbb{E}\{|q_{kl}q_{kl'}^*|\} + \sum_{k'=1}^{L_d}\sum_{k''=1}^{L_d}\sum_{m=1}^{M}\sum_{m=1}^{M}\sqrt{\eta_{mk'}\eta_{m'k''}}\mathbb{E}\{|\mathbf{g}_{mk}^H\hat{\mathbf{g}}_{mk'}\hat{\mathbf{g}}_{m'k''}^H\mathbf{g}_{m'k}|\}.$$

To derive the third term, all possible AP-user combinations are considered. If $k' \neq k'' \neq k$ and $m \neq m'$, $\mathbb{E}\{|\mathbf{g}_{mk}^H\hat{\mathbf{g}}_{mk'}\hat{\mathbf{g}}_{m'k''}^H\mathbf{g}_{m'k}|\} = 0$; If $k' = k'' \neq k$ and $m \neq m'$, $\mathbb{E}\{|\mathbf{g}_{mk}^H\hat{\mathbf{g}}_{mk'}\hat{\mathbf{g}}_{m'k'}^H\mathbf{g}_{m'k}|\} = 0$; For $k' = k'' \neq k$, $m = m'$, $\mathbb{E}\{|\mathbf{g}_{mk}^H\hat{\mathbf{g}}_{mk'}\hat{\mathbf{g}}_{mk'}^H\mathbf{g}_{mk}|\} = \mathbb{E}\{|\mathbf{g}_{mk}^H\hat{\mathbf{g}}_{mk'}|^2\}$. We have

$$\mathbb{E}\{|\mathbf{g}_{mk}^H\hat{\mathbf{g}}_{mk'}|^2\} = \mathbb{E}\{|(\kappa_{mk}^{1/2}\bar{\kappa}_{mk}^{-1/2}\mathbf{g}_{L,mk}^H + \bar{\kappa}_{mk}^{-1/2}\mathbf{g}_{w,mk}^H)\times (\kappa_{mk}^{1/2}\bar{\kappa}_{mk}^{-1/2}\mathbf{g}_{L,mk} + \bar{\kappa}_{mk}^{-1/2}\hat{\mathbf{g}}_{w,mk})|^2\}$$
$$= \kappa_{mk}\bar{\kappa}_{mk}^{-1}\kappa_{mk'}\bar{\kappa}_{mk'}^{-1}\mathbb{E}\{|\mathbf{g}_{L,mk}^H\mathbf{g}_{L,mk'}|^2\} + \bar{\kappa}_{mk}^{-1}\bar{\kappa}_{mk'}^{-1}\times \mathbb{E}\{|\mathbf{g}_{w,mk}^H\hat{\mathbf{g}}_{w,mk'}|^2\} + \kappa_{mk}\bar{\kappa}_{mk}^{-1}\bar{\kappa}_{mk'}^{-1}\mathbb{E}\{|\mathbf{g}_{L,mk}^H\hat{\mathbf{g}}_{w,mk'}|^2\} + \bar{\kappa}_{mk}^{-1}\kappa_{mk'}\bar{\kappa}_{mk'}^{-1}\mathbb{E}\{|\mathbf{g}_{w,mk}^H\mathbf{g}_{L,mk'}|^2\}.$$

The following expectations are derived: $\mathbb{E}\{|\mathbf{g}_{L,mk}^H\mathbf{g}_{L,mk'}|^2\} = \beta_{mk}\beta_{mk'}[\sum_{n=1}^{N_{tx}} e^{j(n-1)\pi\sin(\psi_{mk}^d)}\cdot e^{-j(n-1)\sin(\psi_{mk'}^d)}]^2 \overset{(d)}{=} \beta_{mk}\beta_{mk'}[\phi_{mkk'}e^{j((N_{tx}-1)\pi/2)(\sin(\psi_{mk}^u - \sin(\psi_{mk'}^u))}]^2 = \beta_{mk}\beta_{mk}\phi_{mkk'}^2$, where (d) has used [24, eq. (118)]. Also, $\mathbb{E}\{|\mathbf{g}_{w,mk}^H\hat{\mathbf{g}}_{w,mk'}|^2\} = \beta_{mk'}\nu_{mk'}\mathbb{E}\{\|\mathbf{g}_{w,mk}\|^2\} = \beta_{mk'}\nu_{mk'}\beta_{mk}N_{tx}$, $\mathbb{E}\{|\mathbf{g}_{L,mk}^H\hat{\mathbf{g}}_{w,mk'}|^2\} = \beta_{mk'}\nu_{mk'}\beta_{mk}N_{tx}$ and $\mathbb{E}\{|\mathbf{g}_{w,mk}^H\mathbf{g}_{L,mk'}|^2\} = \beta_{mk'}\beta_{mk}N_{tx}$. Therefore,

$$\mathbb{E}\{|\mathbf{g}_{mk}^H\hat{\mathbf{g}}_{mk'}|^2\} = N_{tx}\beta_{mk}\beta_{mk'}(\nu_{mk'} + \kappa_{mk'} + \kappa_{mk}\nu_{mk'} + \kappa_{mk}\kappa_{mk'}\frac{\phi_{mkk'}^2}{N_{tx}}). \quad (44)$$

Next, if $k' = k'' = k'$ and $m \neq m'$, $\mathbb{E}\{|\mathbf{g}_{mk}^H\hat{\mathbf{g}}_{mk}\hat{\mathbf{g}}_{m'k}^H\mathbf{g}_{m'k}|\} = \mathbb{E}\{|\mathbf{g}_{mk}^H\hat{\mathbf{g}}_{mk}|\}\mathbb{E}\{|\hat{\mathbf{g}}_{m'k}^H\mathbf{g}_{m'k}|\}$. We derive $\mathbb{E}\{|\mathbf{g}_{mk}^H\hat{\mathbf{g}}_{mk}|\} = \mathbb{E}\{|(\hat{\mathbf{g}}_{mk}^H + \tilde{\mathbf{g}}_{mk})\hat{\mathbf{g}}_{mk}|\} = \mathbb{E}\{\|\hat{\mathbf{g}}_{mk}\|^2\}$, where we have used the fact that the estimated and error vectors are uncorrelated. Therefore, $\mathbb{E}\{\|\hat{\mathbf{g}}_{mk}\|^2\} = \mathbb{E}\{\|\kappa_{mk}^{1/2}\bar{\kappa}_{mk}^{-1/2}\mathbf{g}_{L,mk} + \bar{\kappa}_{mk}^{-1/2}\hat{\mathbf{g}}_{w,mk}\|^2\} = \kappa_{mk}\bar{\kappa}_{mk}^{-1}\mathbb{E}\{\mathbf{g}_{L,mk}^H\mathbf{g}_{L,mk}\} + \bar{\kappa}_{mk}^{-1}\mathbb{E}\{\|\hat{\mathbf{g}}_{w,mk}\|^2\}$, where we exploit the zero-mean property of estimated white channel. $\mathbb{E}\{\mathbf{g}_{L,mk}^H\mathbf{g}_{L,mk}\} = \beta_{mk}\sum_{n=1}^{N_{tx}} e^{j(n-1)\pi\sin(\psi_{mk}^u)}\cdot e^{-j(n-1)\pi\sin(\psi_{mk}^u)} = \beta_{mk}N_{tx}$ and $\mathbb{E}\{\|\hat{\mathbf{g}}_{w,mk}\|^2\} = \beta_{mk}\nu_{mk}N_{tx}$. We have $\mathbb{E}\{\|\hat{\mathbf{g}}_{mk}\|^2\} = \bar{\kappa}_{mk}^{-1}\beta_{mk}N_{tx}(\kappa_{mk} + \nu_{mk})$. Similarly, $\mathbb{E}\{|\hat{\mathbf{g}}_{m'k}^H\mathbf{g}_{m'k}|\} = \bar{\kappa}_{m'k}^{-1}\beta_{m'k}N_{tx}(\kappa_{m'k} + \nu_{m'k})$. Thus,

$$\mathbb{E}\{|\mathbf{g}_{mk}^H\hat{\mathbf{g}}_{mk}\hat{\mathbf{g}}_{m'k}^H\mathbf{g}_{m'k}|\} = N_{tx}^2\bar{\kappa}_{mk}^{-1}\beta_{mk}\bar{\kappa}_{m'k}^{-1}\beta_{m'k}(\kappa_{mk} + \nu_{mk})(\kappa_{m'k} + \nu_{m'k}). \quad (45)$$

Finally, for $k' = k'' = k$ and $m = m'$, $\mathbb{E}\{|\mathbf{g}_{mk}^H\hat{\mathbf{g}}_{mk}|^2\} = \mathbb{E}\{|\tilde{\mathbf{g}}_{mk}^H\hat{\mathbf{g}}_{mk}|^2\} + \mathbb{E}\{\|\hat{\mathbf{g}}_{mk}\|^4\}$. We derive $\mathbb{E}\{|\tilde{\mathbf{g}}_{mk}^H\hat{\mathbf{g}}_{mk}|^2\} = \tilde{\beta}_{mk}\mathbb{E}\{\|\hat{\mathbf{g}}_{mk}\|^2\} = N_{tx}\tilde{\beta}_{mk}\bar{\kappa}_{mk}^{-1}\beta_{mk}(\kappa_{mk} + \nu_{mk})$ and

$$\mathbb{E}\{\|\hat{\mathbf{g}}_{mk}\|^4\} = \mathbb{E}\{|(\kappa_{mk}^{1/2}\bar{\kappa}_{mk}^{-1/2}\mathbf{g}_{L,mk}^H + \bar{\kappa}_{mk}^{-1/2}\hat{\mathbf{g}}_{w,mk}^H)(\kappa_{mk}\times \bar{\kappa}_{mk}^{-1}\mathbf{g}_{L,mk} + \bar{\kappa}_{mk}^{-1}\hat{\mathbf{g}}_{w,mk})|^2\} \overset{(c)}{=} \kappa_{mk}^2\bar{\kappa}_{mk}^{-2}\mathbb{E}\{|\mathbf{g}_{L,mk}^H\mathbf{g}_{L,mk}|^2\} + \kappa_{mk}\bar{\kappa}_{mk}^{-2}\mathbb{E}\{|\mathbf{g}_{L,mk}^H\hat{\mathbf{g}}_{w,mk}|^2\} + \kappa_{mk}\bar{\kappa}_{mk}^{-2}\mathbb{E}\{|\hat{\mathbf{g}}_{w,mk}^H\mathbf{g}_{L,mk}|^2\} + \bar{\kappa}_{mk}^{-2}\mathbb{E}\{\|\hat{\mathbf{g}}_{w,mk}\|^4\} + \kappa_{mk}\bar{\kappa}_{mk}^{-2}\mathbb{E}\{|\mathbf{g}_{L,mk}^H\mathbf{g}_{L,mk}\hat{\mathbf{g}}_{w,mk}^H\hat{\mathbf{g}}_{w,mk}|\} + \kappa_{mk}\bar{\kappa}_{mk}^{-2}\mathbb{E}\{|\hat{\mathbf{g}}_{w,mk}^H\hat{\mathbf{g}}_{w,mk}\mathbf{g}_{L,mk}^H\mathbf{g}_{L,mk}|\}. \quad (46)$$

Note that in (c), we remove the terms with zero mean. From (46), we can derive the following expectations: $\mathbb{E}\{|\mathbf{g}_{L,mk}^H\mathbf{g}_{L,mk}|^2\} = \beta_{mk}^2N_{tx}^2$, $\mathbb{E}\{|\mathbf{g}_{L,mk}^H\hat{\mathbf{g}}_{w,mk}|^2\} = \beta_{mk}^2\nu_{mk}N_{tx}$, and $\mathbb{E}\{|\mathbf{g}_{L,mk}^H\mathbf{g}_{L,mk}\hat{\mathbf{g}}_{w,mk}^H\hat{\mathbf{g}}_{w,mk}|\} = \mathbb{E}\{|\mathbf{g}_{L,mk}^H\mathbf{g}_{L,mk}|\}\mathbb{E}\{|\hat{\mathbf{g}}_{w,mk}^H\hat{\mathbf{g}}_{w,mk}|\} = N_{tx}^2\beta_{mk}^2\nu_{mk}$. Similarly, $\mathbb{E}\{|\hat{\mathbf{g}}_{w,mk}^H\hat{\mathbf{g}}_{w,mk}\mathbf{g}_{L,mk}^H\mathbf{g}_{L,mk}|\} = N_{tx}^2\beta_{mk}^2\nu_{mk}$.

Using [43, Lemma 2.9], $\mathbb{E}\{\|\hat{\mathbf{g}}_{w,mk}\|^4\} = \beta_{mk}^2\nu_{mk}^2N_{tx}(N_{tx} + 1)$. Thus, $\mathbb{E}\{\|\hat{\mathbf{g}}_{mk}\|^4\} = \bar{\kappa}_{mk}^{-2}\beta_{mk}^2(\kappa_{mk}^2N_{tx}^2 + \nu_{mk}^2N_{tx}^2 + \nu_{mk}^2N_{tx} + 2\kappa_{mk}\nu_{mk}N_{tx} + 2\kappa_{mk}\nu_{mk}N_{tx}^2)$. Therefore, $\mathbb{E}\{|\mathbf{g}_{mk}^H\hat{\mathbf{g}}_{mk}|^2\}$ gives the solution

$$\mathbb{E}\{|\mathbf{g}_{mk}^H\hat{\mathbf{g}}_{mk}|^2\} = N_{tx}\tilde{\beta}_{mk}\bar{\kappa}_{mk}^{-1}\beta_{mk}(\kappa_{mk} + \nu_{mk}) + \bar{\kappa}_{mk}^{-2}\beta_{mk}^2\times (\kappa_{mk}^2N_{tx}^2 + \nu_{mk}^2N_{tx}^2 + \nu_{mk}^2N_{tx} + 2\kappa_{mk}\nu_{mk}N_{tx} + 2\kappa_{mk}\nu_{mk}N_{tx}^2) = \beta_{mk}^2\bar{\kappa}_{mk}^{-2}[N_{tx}(\nu_{mk} + \kappa_{mk} + \nu_{mk}\kappa_{mk}) + N_{tx}^2(\kappa_{mk}^2 + \nu_{mk}^2 + 2\kappa_{mk}\nu_{mk})], \quad (47)$$

where we have used $\tilde{\beta}_{mk} = \beta_{mk}\kappa_{mk}^{-1} - \hat{\beta}_{mk}$.

Finally, we consider $\mathbb{E}\{|q_{kl}q_{kl'}|\}$ from above. If $l' \neq l$, $\mathbb{E}\{|q_{kl}q_{kl'}|\} = 0$ and for $l' = l$, $\mathbb{E}\{|q_{kl}|^2\} = \gamma_{kl}^2$. Using (44),

(45), and (47), the QN at the k-th DL user is written as

$$\tilde{Z}_k^d = \Big[N_{tx}\sum_{k'\neq k}^{L_d}\sum_{m=1}^{M}\eta_{mk'}\beta_{mk}\beta_{mk'}\Big(\kappa_{mk}\nu_{mk'}+\nu_{mk'}+\kappa_{mk'} + \frac{\kappa_{mk}\kappa_{mk'}\phi_{mkk'}^2}{N_{tx}}\Big)+N_{tx}\sum_{m=1}^{M}\eta_{mk}\beta_{mk}^2\bar{\kappa}_{mk}^{-2}\Big(\nu_{mk}\kappa_{mk}+\nu_{mk} + \kappa_{mk}\Big)+N_{tx}^2\sum_{m=1}^{M}\sum_{m'=1}^{M}\sqrt{\eta_{mk}\eta_{m'k}}\bar{\kappa}_{mk}^{-1}\beta_{mk}\bar{\kappa}_{m'k}^{-1}\beta_{m'k}\Big(\kappa_{mk}\times \kappa_{m'k}+\nu_{mk}\nu_{m'k}+\kappa_{mk}\nu_{m'k}+\kappa_{m'k}\nu_{mk}\Big)+\sum_{l=1}^{L_u}p_{u,l}\gamma_{kl}^2\Big] \times(\varepsilon_k-\varepsilon_k^2). \tag{48}$$

This completes the proof.

REFERENCES

[1] S. Zhou, M. Zhao, X. Xu, J. Wang, and Y. Yao, "Distributed wireless communication system: A new architecture for future public wireless access," *IEEE Commun. Mag.*, vol. 41, no. 3, pp. 108–113, Mar. 2003.

[2] Z. Chen and E. Björnson, "Channel hardening and favorable propagation in cell-free massive MIMO with stochastic geometry," *IEEE Trans. Commun.*, vol. 66, no. 11, pp. 5205–5219, Nov. 2018.

[3] H. Q. Ngo, A. Ashikhmin, H. Yang, E. G. Larsson, and T. L. Marzetta, "Cell-free massive MIMO versus small cells," *IEEE Trans. Wireless Commun.*, vol. 16, no. 3, pp. 1834–1850, Mar. 2017.

[4] H. Q. Ngo, L.-N. Tran, T. Q. Duong, M. Matthaiou, and E. G. Larsson, "On the total energy efficiency of cell-free massive MIMO," *IEEE Trans. Green Commun. Netw.*, vol. 2, no. 1, pp. 25–39, Mar. 2018.

[5] L. D. Nguyen, T. Q. Duong, H. Q. Ngo, and K. Tourki, "Energy efficiency in cell-free massive MIMO with zero-forcing precoding design," *IEEE Commun. Lett.*, vol. 21, no. 8, pp. 1871–1874, Apr. 2017.

[6] Ö. Özdogan, E. Björnson, and J. Zhang, "Performance of cell-free massive MIMO with Rician fading and phase shifts," *IEEE Trans. Wireless Commun.*, vol. 18, no. 11, pp. 5299–5315, Aug. 2019.

[7] Z. Wang, J. Zhang, E. Björnson, and B. Ai, "Uplink performance of cell-free massive MIMO over spatially correlated Rician fading channels," *IEEE Commun. Lett.*, vol. 25, no. 4, pp. 1348–1352, Apr. 2021.

[8] H. Q. Ngo, H. A. Suraweera, M. Matthaiou, and E. G. Larsson, "Multipair full-duplex relaying with massive arrays and linear processing," *IEEE J. Sel. Areas Commun.*, vol. 32, no. 9, pp. 1721–1737, Sep. 2014.

[9] D. Kim, H. Lee, and D. Hong, "A Survey of in-band full-duplex transmission: From the perspective of PHY and MAC layers," *IEEE Commun. Surveys Tut.*, vol. 17, no. 4, pp. 2017 –2046, Feb. 2015.

[10] Vu et al., "Full-duplex cell-free massive MIMO," in *Proc. IEEE Int. Conf. Commun. (ICC)*, pp. 1–6, May 2019.

[11] D. Wang, M. Wang, P. Zhu, J. Li, J. Wang, and X. You, "Performance of network-assisted full-duplex for cell-free massive MIMO," *IEEE Trans. Commun.*, vol. 68, no. 3, pp. 1464–1478, Mar. 2020.

[12] Nguyen et al., "On the spectral and energy efficiencies of full-duplex cell-free massive MIMO," *IEEE J. Sel. Areas Commun.*, vol. 38, no. 8, pp. 1698–1718, Jun. 2020.

[13] J. Mo and R. W. Heath, "Limited feedback in single and multi-user MIMO systems with finite-bit ADCs," *IEEE Trans. Wireless Commun.*, vol. 17, no. 5, pp. 3284–3297, May 2018.

[14] A. Alkhateeb, J. Mo, N. Gonzalez-Prelcic, and R. W. Heath, "MIMO precoding and combining solutions for millimeter-wave systems," *IEEE Commun. Mag.*, vol. 52, no. 12, pp. 122–131, Dec. 2014.

[15] X. Hu, C. Zhong, X. Chen, W. Xu, H. Lin, and Z. Zhang, "Cell-free massive MIMO systems with low resolution ADCs," *IEEE Trans. Commun.*, vol. 67, no. 10, pp. 6844–6857, Oct. 2019.

[16] P. Anokye, R. K. Ahiadormey, and K.-J. Lee, "Full-duplex cell-free massive MIMO with low-resolution ADCs," *IEEE Trans. Veh. Technol.*, vol. 70, no. 11, pp. 12179–12184, Nov. 2021.

[17] S.-H. Park et. al., "Optimizing pilots and analog processing for channel estimation in cell-free massive MIMO with one-bit ADCs," in *Proc. IEEE Int. Workshop on Sign. Process. Adv. Wireless Commun. (SPAWC)*, pp. 1–5, Jun. 2018.

[18] Y. Zhang, H. Cao, M. Zhou, X. Qiao, and L. Yang, "Rate analysis of cell-free massive MIMO with one-bit ADCs and DACs," in *Proc. IEEE Ann. Int. Sym. PIMRC*, pp. 1–6, Nov. 2019.

[19] Y. Zhang, L. Yang, and H. Zhu, "Cell-free massive MIMO systems with low-resolution ADCs: The Rician fading case," *IEEE Syst. J.*, vol. 16, no. 1, pp. 1471–1482, Mar. 2022.

[20] Y. Zhang, M. Zhou, H. Cao, L. Yang, and H. Zhu, "On the performance of cell-free massive MIMO with mixed-ADC under Rician fading channels," *IEEE Commun. Lett.*, vol. 24, no. 1, pp. 43–47, Jan. 2020.

[21] Anokye et al., "On the sum-rate of heterogeneous networks with low-resolution ADC quantized full-duplex massive MIMO-enabled backhaul," *IEEE Wireless Commun. Lett.*, vol. 8, no. 2, pp. 452–455, Apr. 2019.

[22] Anokye et al., "Low-resolution ADC quantized full-duplex massive MIMO-enabled wireless backhaul in heterogeneous networks over Rician channels," *IEEE Trans. Wireless Commun.*, vol. 19, no. 8, pp. 5503–5517, Aug. 2020.

[23] E. Larson, F. Tufvesson, O. Edfors, and T. Marzetta, "Massive MIMO for next generation wireless systems," *IEEE Commun. Mag.*, vol. 52, no. 2, pp. 186–195, Feb. 2014.

[24] Q. Zhang, S. Jin, K. Wong, H. Zhu, and M. Matthaiou, "Power scaling of uplink massive MIMO systems with arbitrary-rank channel means," *IEEE J. Sel. Topics Signal Process.*, vol. 8, no. 5, pp. 966–981, Oct. 2014.

[25] R. O. Schmidt, *A signal subspace approach to multiple emitter location and spectral estimation*. PhD thesis, Standford University, Standford, CA, USA, 1981.

[26] R. Roy and T. Kailath, "ESPRIT-estimation of signal parameters via rotational invariance techniques," vol. 37, no. 7, pp. 984–995, 1989.

[27] S. Wang, Y. Liu, W. Zhang, and H. Zhang, "Achievable rates of full-duplex massive MIMO relay systems over Rician fading channels," *IEEE Trans. Veh. Technol.*, vol. 66, no. 11, pp. 9825–9837, Nov. 2017.

[28] T. Riihonen, S. Werner, and R. Wichman, "Hybrid full-duplex/half-duplex relaying with transmit power adaptation," *IEEE Trans. Wireless Commun.*, vol. 10, no. 9, pp. 3074–3085, Sep. 2011.

[29] K. Roth and J. A. Nossek, "Achievable rate and energy efficiency of hybrid and digital beamforming receivers with low resolution ADC," *IEEE J. Sel. Areas Commun.*, vol. 35, no. 9, pp. 2056–2068, Sep. 2017.

[30] J. Mo, A. Alkhateeb, S. Abu-Surra, and R. W. Heath, "Hybrid architectures with few-bit ADC receivers: Achievable rates and energy-rate tradeoffs," *IEEE Trans. Wireless Commun.*, vol. 16, no. 4, pp. 2274–2287, 2017.

[31] Y. Zhang, Y. Cheng, M. Zhou, L. Yang, and H. Zhu, "Analysis of uplink cell-free massive MIMO system with mixed-ADC/DAC receiver," *IEEE Syst. J.*, vol. 15, no. 4, pp. 5162–5173, Dec. 2021.

[32] J. Zhang, L. Dai, Z. He, B. Ai, and O. A. Dobre, "Mixed-ADC/DAC multipair massive MIMO relaying systems: Performance analysis and power optimization," *IEEE Trans. Commun.*, vol. 67, no. 1, pp. 140–153, Jan. 2019.

[33] B. D. Antwi-Boasiako, R. K. Ahiadormey, P. Anokye, and K.-J. Lee, "On the performance of massive MIMO full-duplex relaying with low-resolution ADCs," *IEEE Commun. Lett.*, vol. 26, no. 6, pp. 1259–1263, 2022.

[34] T. Liu, J. Tong, J. Yuan, J. Xi, H. Wang, and L. Zhao, "Massive MIMO with group SIC receivers and low-resolution ADCs over Rician fading channels," *IEEE Trans. Veh. Technol.*, pp. 1–17, 2022.

[35] S. S. Christensen, R. Agarwal, E. De Carvalho, and J. M. Cioffi, "Weighted sum-rate maximization using weighted MMSE for MIMO-BC beamforming design," *IEEE Trans. Wireless Commun.*, vol. 7, no. 12, pp. 4792–4799, Dec. 2008.

[36] T. Van Chien, C. Mollén, and E. Björnson, "Large-scale-fading decoding in cellular massive MIMO systems with spatially correlated channels," *IEEE Trans. Commun.*, vol. 67, no. 4, pp. 2746–2762, Apr. 2019.

[37] A. C. Cirik, R. Wang, Y. Hua, and M. Latva-aho, "Weighted sum-rate maximization for full-duplex MIMO interference channels," *IEEE Trans. Commun.*, vol. 63, no. 3, pp. 801–815, Mar. 2015.

[38] S. Boyd, N. Parikh, E. Chu, B. Peleato, and J. Eckstein, "Distributed optimization and statistical learning via the alternating direction method of multipliers," *Foundation and Trends in Machine Learning*, vol. 3, no. 1, pp. 1–122, 2010.

[39] "Technical specification group radio access network; Spatial channel model for multiple input multiple output (MIMO) simulations," techreport V16.0.0, 3rd Generation Partnership Project, Jul. 2020.

[40] R. Mendez-Rial, C. Rusu, N. Gonzalez-Prelcic, A. Alkhateeb, and R. W. H. Jr, "Hybrid MIMO architectures for millimeter wave communications: Phase shifters or switches," *IEEE Access*, vol. 4, pp. 247–267, Jan. 2016.

[41] J. Zhang, L. Dai, Z. He, S. Jin, and X. Li, "Performance analysis of mixed-ADC massive MIMO systems over Rician fading channels," *IEEE J. Sel. Areas Commun.*, vol. 35, no. 6, pp. 1327–1338, Jun. 2017.

[42] Abbas et al., "Millimeter wave receiver efficiency: A comprehensive comparison of beamforming schemes with low resolution ADCs," *IEEE Trans. Wireless Commun.*, vol. 16, no. 12, pp. 8131–8146, Dec. 2017.

[43] A. Tulino and S. Verdu, *Random matrix theory and wireless communication*, vol. 1. Now Publishers Inc., foundation and trends in communications and information theory ed., June 2004.